# Impact of a moderate volcanic eruption on chemistry in the lower stratosphere: balloon-borne observations and model calculations

Gwenaël Berthet[1], Fabrice Jégou[1], Valéry Catoire[1], Gisèle Krysztofiak[1], Jean-Baptiste Renard[1], Adam E. Bourassa[2], Doug A. Degenstein[2], Colette Brogniez[3], Marcel Dorf[4], Sebastian Kreycy[4], Klaus Pfeilsticker[4], Bodo Werner[4], Franck Lefèvre[5], Tjarda J. Roberts[1], Thibaut Lurton[1], Damien Vignelles[1], Nelson Bègue[6], Quentin Bourgeois[7], Daniel Daugeron[1], Michel Chartier[1], Claude Robert[1], Bertrand Gaubicher[1], and Christophe Guimbaud[1]

[1]Laboratoire de Physique et Chimie de l'Environnement et de l'Espace (LPC2E), Université d'Orléans, CNRS UMR7328, Orléans, France
[2]Institute of Space and Atmospheric Studies, University of Saskatchewan, Saskatoon, Canada
[3]Laboratoire d'Optique Atmosphérique, Université Lille 1 Sciences et Technologies, CNRS UMR8518, Villeneuve d'Ascq, France
[4]Institute of Environmental Physics, University of Heidelberg, Heidelberg, Germany
[5]Laboratoire Atmosphères Milieux Observations Spatiales, UPMC, Université Paris 06, Université Versailles Saint Quentin, CNRS UMR8190, LATMOS-IPSL, Paris, France
[6]Laboratoire de l'Atmosphère et des Cyclones, UMR8105 CNRS, Université de la Réunion, France
[7]Department of Meteorology and Bolin Centre for Climate Research, Stockholm University, Stockholm, Sweden

## Abstract.

The major volcanic eruption of Mount Pinatubo in 1991 has been shown to have significant effects on stratospheric chemistry and ozone depletion even at mid-latitudes. Since then, only "moderate" but recurrent volcanic eruptions have modulated the stratospheric aerosol loading and are assumed to be one cause for the reported increase in the global aerosol content over the past 15 years. This particular enhanced aerosol context raises questions about the effects on stratospheric chemistry which depend on the latitude, altitude and season of injection. In this study, we focus on the mid-latitude Sarychev volcano eruption in June 2009 which injected 0.9 Tg of sulfur dioxide (about 20 times less than Pinatubo) in a lower stratosphere mainly governed by high stratospheric temperatures. Together with in situ measurements of aerosol amounts, we analyse high-resolution in situ and/or remote-sensing observations of $NO_2$, $HNO_3$ and BrO from balloon-borne infrared and UV-visible spectrometers launched in Sweden in August-September 2009. It is shown that differences between observations and three-dimensional (3D) Chemistry-Transport Model (CTM) outputs are not due to transport calculation issues but rather reflect the chemical impact of the volcanic plume below 19 km altitude. Good measurement-model agreement is obtained when the CTM is driven by volcanic aerosol loadings derived from in situ or space-borne data. As a result of enhanced $N_2O_5$ hydrolysis in the Sarychev volcanic aerosol conditions, the model calculates reductions of ~45% and increases of ~11% in $NO_2$ and $HNO_3$ amounts respectively over the August-September 2009 period. The decrease in $NO_x$ abundances is limited due to the expected saturation effect for high aerosol loadings. The links between the various chemical catalytic cycles involving chlorine, bromine, nitrogen and $HO_x$ compounds in the lower stratosphere are discussed. The increased BrO amounts (~22%) compare rather well with the balloon-borne observations when volcanic aerosol levels are accounted for in the CTM and appear to be mainly controlled by the coupling with nitrogen chemistry rather than by enhanced $BrONO_2$ hydrolysis. We show that the chlorine partitioning is significantly controlled by enhanced $BrONO_2$ hydrolysis. However simulated effects of the Sarychev eruption on chlorine activation are very limited in the high temperature conditions in the stratosphere at the period considered, inhibiting the effect of $ClONO_2$ hydrolysis. As a consequence, the simulated chemical ozone loss due to the Sarychev aerosols is low with a reduction of -22 ppbv (-1.5%) of the ozone budget around 16 km. This is at least 10 times lower than the maximum ozone depletion from

chemical processes (up to -20%) reported in the northern hemisphere lower stratosphere over the first year following the Pinatubo eruption. This study suggests that moderate volcanic eruptions have limited chemical effects when occurring at mid-latitudes (restricted residence times) and outside winter periods (high temperature conditions). However, among the other reported moderate eruptions it would be of interest to investigate longer lasting tropical volcanic plumes or sulfur injections in the wintertime low temperature conditions.

# 1. Introduction

In the stratosphere, the photo-oxidation of $N_2O$ is the main source of the total nitrogen species ($NO_y$). About 97% of the stratospheric $NO_y$ budget can be explained by the NO, $NO_2$, $HNO_3$, $ClONO_2$, and $N_2O_5$ compounds and the partitioning between reactive and reservoir nitrogen species is an important issue in stratospheric ozone chemistry (e.g. Wetzel et al., 2002; Brohede et al., 2008). Nitrogen oxides ($NO_x$ = NO + $NO_2$) are major catalysts responsible for significant ozone destruction in the middle stratosphere. In the gas phase, $NO_x$ interacts with the hydrogen and halogen species in catalytic cycles affecting ozone loss rates in the lower stratosphere (e.g. Portmann et al., 1999; Salawitch et al., 2005). Therefore $NO_x$ can also buffer the ozone destruction by halogenated compounds through the formation of $ClONO_2$ and $BrONO_2$ (e.g. Rivière et al., 2004). The $HNO_3$ reservoir is formed from $NO_x$ indirectly via the hydrolysis of $N_2O_5$ on liquid sulfate aerosols:

$$N_2O_5 + H_2O_{(aq)} \rightarrow 2\ HNO_3 \quad (1)$$

It has been shown that models need to include reaction (1) to better reproduce observations of $NO_y$ partitioning at mid-latitude for background aerosol conditions (i.e. in volcanically quiescent periods) in the lower stratosphere (Rodriguez et al., 1991; Granier and Brasseur, 1992; Fahey et al., 1993; Webster et al., 1994; Salawitch et al., 1994b; Sen et al., 1998). This reaction tends to decrease $NO_x$ amounts and reduces the ozone loss efficiency associated with the $NO_x$ catalytic cycle as the less reactive nitrogen reservoir $HNO_3$ is formed (e.g. Rodriguez et al., 1991; Weisenstein, 1991; McElroy et al., 1992). Reaction (1) is fairly insensitive to temperature and has the potential to greatly reduce reactive nitrogen globally, even under background aerosol conditions.

The hydrolysis of $ClONO_2$ can be expressed by:

$$ClONO_2 + H_2O_{(aq)} \rightarrow\ HNO_3 + HOCl \quad (2)$$

It results in additional formation of $HNO_3$ on sulfate aerosols and to the formation of reactive chlorine in the sunlight where HOCl is rapidly photolyzed releasing Cl radicals (e.g. Hofmann and Solomon, 1989; Prather, 1992; McElroy et al., 1992). This heterogeneous reaction is highly dependent on the water content in the aerosols and has been shown to be of considerable importance in determining the abundance of active chlorine available to destroy ozone under some conditions, i.e. for temperatures typically below 210-215 K and where $HNO_3$ photolysis rates are slow (typically in winter at high latitudes), (e.g. Hanson et al., 1994; Tie et al., 1994; Borrmann et al., 1997). However, for higher temperatures the $ClONO_2$ hydrolysis is not expected to be significant enough to compete with reaction (1) on the $NO_y$ partitioning under these conditions (Fahey et al., 1993; Cox et al., 1994; Sen et al., 1998). Also, the reaction,

$$ClONO_2 + HCl_{(aq)} \rightarrow\ HNO_3 + Cl_2 \quad (3)$$

of $ClONO_2$ with dissolved HCl in sulfuric acid droplets has negligible effects on chlorine activation at such temperatures (Hanson et al., 1994; Borrmann et al., 1997).

Some works also suggest that the hydrolysis of $BrONO_2$,

$$BrONO_2 + H_2O_{(aq)} \rightarrow\ HNO_3 + HOBr \quad (4)$$

on background sulfate aerosols also plays a significant role in ozone depletion in the lower stratosphere with rates almost independent of temperature making this reaction efficient at all latitudes and for all seasons (Hanson and Ravishankara, 1995; Hanson et al., 1996; Lary et al., 1996; Randeniya et al., 1997; Erle et al., 1998).

After large volcanic eruptions, the aerosol loading in the stratosphere and the surface area densities (hereafter SAD) available for reaction (1) to occur are dramatically enhanced (e.g. Deshler et al., 2003). As a result, the amount of ozone-depleting $NO_x$ is strongly reduced (e.g. Prather, 1992; Johnston et al., 1992; Fahey, 1993; Mills et al., 1993; Solomon et al., 1994; Kondo et al., 1997; Sen et al., 1998; Dhomse et al., 2015) whereas $HNO_3$ amounts increase (Koike et al., 1993; Webster et al., 1994; Koike et al.,

1994; Rinsland et al., 2003) as shown for the Pinatubo aerosols. Different chemical impacts on stratospheric ozone are expected depending on the altitude. In the middle stratosphere (above ~30 hPa) where ozone loss is dominated by $NO_x$, the presence of volcanic aerosols can result in layers of increased net production of ozone due to the suppression of the $NO_x$ cycle by the $N_2O_5$ hydrolysis (Hofmann et al., 1994; Bekki and Pyle, 1994; Tie and Brasseur, 1995). In the lower stratosphere, halogen ($ClO_x$ and $BrO_x$) and hydrogen ($HO_x$) radicals play a dominant role in ozone depletion and their abundances, which depend on $NO_x$ levels, are increased (in particular for halogen species, as the rate of gas-phase conversion of ClO into the $ClONO_2$ reservoir is reduced), resulting in an enhanced catalyzed ozone loss (McElroy et al., 1992; Granier and Brasseur, 1992; Brasseur and Granier, 1992; Hofmann et al., 1994; McGee et al., 1994; Bekki and Pyle, 1994; Salawitch et al., 1994a; 2005; Tie et al., 1994; Solomon et al., 1996; Solomon, 1999).

However, the $NO_x$-to-$HNO_3$ conversion by reaction (1) shows saturation as the aerosol SAD increases because the amount of $N_2O_5$ present in the stratosphere is limited by its production rate by the gaseous reaction $NO_2 + NO_3$ (Fahey, 1993; Prather, 1992; Mills et al., 1993; Tie et al., 1994; Solomon et al., 1996; Kondo et al., 1997; Sen et al., 1998). Consequently, ozone loss rates are expected to be limited because the saturation of the $NO_x/NO_y$ response to the aerosol increase dampens the increase in $ClO/Cl_y$ (Fahey et al., 1993; Tie et al., 1994). Reaction (2) does not show such a rapid saturation resulting in enhanced ozone depletion by chlorine catalytic cycles in cold air masses as the aerosol loading increases (Fahey et al., 1993). The $BrONO_2$ hydrolysis through reaction (4) is primarily dependent on the aerosol loading and is enhanced in periods of high volcanic aerosol loading. The resulting increase of $BrO_x$ and $HO_x$ radical concentrations and decrease in HCl (due to enhanced OH) accompanied by an increase in $ClO_x$ radicals is expected to give further ozone loss in the lower stratosphere at all latitudes and seasons (Lary et al., 1996).

In periods following major eruptions, the year-to-year variability in stratospheric ozone at northern mid-latitudes appears closely linked to dynamical changes induced by the volcanic aerosol radiative perturbation (e.g. Telford et al., 2009; Aquila et al., 2013) and to changes in chlorine partitioning (e.g. Solomon et al., 1999; Chipperfield, 1999). Effects on stratospheric chemistry are expected in periods of elevated chlorine levels from anthropogenic activities (Tie and Brasseur, 1995; Solomon et al., 1996). In the past decade no event comparable to the 1991 Pinatubo or 1982 El Chichon eruptions was observed. However, several volcanic eruptions, though of much lesser amplitude, impacted the aerosol burden in the lower stratosphere over periods of months (Vernier et al., 2011). These "moderate" eruptions have occurred in a period of still high chlorine loading with potential impact on stratospheric ozone chemistry. Their effects depend on the amount of released $SO_2$ and on latitudes and altitudes of injection which directly influence aerosol residence times. The season of the eruption is also important for photochemical processes which are directly connected to temperatures and solar illumination.

The goal of this paper is to show how such moderate eruptions are likely to modify the chemical balance of the northern hemisphere lower stratosphere at periods excluding wintertime/springtime halogen-activating photochemistry. We specifically focus on the eruption of the Sarychev volcano on 15 and 16 June 2009 which injected 0.9 Tg of sulfur dioxide in the lower stratosphere (Clarisse et al., 2012) resulting in enhanced sulfate aerosol loading up to 19 km, for a period of about 8 months ending before winter (Haywood et al., 2010; Kravitz et al., 2011; O'Neill et al., 2012; Jégou et al., 2013).

The approach consists in analysing some key aspects of lower stratospheric chemistry and ozone loss in a context of high aerosol surface area densities and high stratospheric temperatures using balloon-borne observations conducted in August-September 2009 from Kiruna/Esrange in Sweden (67.5°N, 21.0°E) within the frame of the STRAPOLETE project. To our knowledge we show here the first high-resolution in situ observations of chemical compounds obtained within the volcanic aerosol plume of a moderate eruption. We show that at the period on which the study is focused $N_2O_5$ has reformed and the role of its hydrolysis becomes important again after the sunlit summer period justifying the use of these balloon data for the investigation of heterogeneous processes. Aerosol-constrained simulations using a 3D Chemistry Transport Model (CTM) are compared to the observations. These model calculations ignore possible dynamical effects induced by the volcanic aerosols but are used to estimate the amplitude of the chemical impacts and ozone loss with some comparisons with the post-Pinatubo eruption period.

# 2. Methodology

## 2.1 Balloon-borne observations

Our study is based on in situ and remote-sensing balloon-borne observations obtained during summer 2009 in Northern Sweden. More details about the instrument descriptions and retrieval techniques are given in the Appendix and in the references. Data can be found at http://www.pole-ether.fr.

### 2.1.1 In situ observations

Aerosol in situ measurements have been performed by the STAC (Stratospheric and Tropospheric Aerosol Counter) instrument which is an optical particle counter providing aerosol size distributions (Ovarlez and Ovarlez, 1995; Renard et al., 2008). This instrument has been used in a number of studies dedicated to the quantification of the aerosol content in the stratosphere at various locations and seasons (e.g. Renard et al., 2002; Renard et al., 2010). Eight vertical aerosol concentration profiles have been obtained between August and September 2009 as reported by Jégou et al. (2013).

Our study presents in situ vertical profiles of the $N_2O$, $NO_2$ and $HNO_3$ gases as observed by the SPIRALE (French acronym for SPectroscopie InfraRouge d'Absorption par Lasers Embarqués) infrared absorption spectrometer (Moreau et al., 2005) from two balloon flights. Firstly, the measurements during the 7 August 2009 flight (further on called SPIRALE-07082009) were conducted between 02:00 UT (04:00 local time) and 03:20 UT (05:20 local time) corresponding to altitudes of 14 km and 34 km respectively. The position of the balloon varied from 67.72°N-21.40°E to 67.63°N-20.92°E during the ascent. Secondly, for the SPIRALE balloon flight on 24 August 2009 (further on called SPIRALE-24082009), the measurements started at 21:00 UT (23:00 local time) at an altitude of 14 km and the maximum altitude of 34 km was reached at 22:30 UT (00:30 local time). The measurement position remained rather constant during the ascent with a displacement of the balloon from 67.91°N-21.09°E to 67.86°N-20.94°E. The data used in this study are averaged over a vertical range of 250 m (corresponding to ~1 minute of measurements).

### 2.1.2 Remote-sensing observations

Since 1996 stratospheric $NO_2$ and BrO have been measured by solar occultation by the DOAS balloon-borne instrument using the so-called Differential Optical Absorption Spectroscopy (DOAS) technique (e.g. Platt, 1994; Stutz and Platt, 1996; Ferlemann et al., 2000). The details of the vertical profile retrieval can be found in Butz et al. (2006) for $NO_2$ and in Harder et al. (1998), Aliwell et al. (2002), Dorf et al. (2006b) and Kreycy et al. (2013) for BrO. In our study we use the DOAS profile recorded in the stratosphere during the balloon ascent on 7 September 2009 between 15:15 UT (17:15 local time) and 16:35 UT (18:35 local time), corresponding to altitudes of 10 km and 30 km respectively.

The SALOMON (French acronym for "Spectroscopie d'Absorption Lunaire pour l'Observation des Minoritaires Ozone et $NO_x$") balloon-borne UV-visible spectrometer also uses the DOAS method to derive the mixing ratio profile of $NO_2$ (Renard et al., 2000; Berthet et al., 2002). SALOMON was initially based on the lunar occultation technique but on 25 August 2009, we flew a new version also able to use the Sun as direct light source to derive BrO amounts. The profiles used in this study have been obtained on 25 August 2009 during solar occultation between 18:50 UT (20:50 local time) and 19:30 UT (21:30 local time). The float altitude was of 33 km and the position of the tangent point varied from 71.0°N-13.3°E to 71.4°N-12.6°E for altitudes below 19 km which are the main focus of our study as a result of the presence of the volcanic aerosols.

Variations of solar zenith angle (SZA) along solar occultation lines of sight and associated concentration variations are likely to impact the retrieved vertical profiles near sunrise and sunset especially below 20 km (Newchurch et al., 1996; Ferlemann et al., 1998). Some works propose to use a photochemical model to correct for this effect (e.g. Harder et al., 2000; Butz et al., 2006) depending on the considered chemical compound, the observation geometry (i.e. balloon ascent or occultation) and daytime (SZA variation). Typically, concentrations are converted to values expected at 90° SZA.

In our study, the $NO_2$ profile from the SALOMON instrument recorded on 25 August 2009 from a typical solar occultation at constant float altitude is not photochemically corrected since conversion to 90° SZA conditions results in differences of less than 6%, in agreement with the work of Payan et al. (1999). The $NO_2$ vertical profile observed by the DOAS instrument was recorded on 7 September 2009 with a different observation geometry, i.e. during the balloon ascent. In this case applying a photochemical correction gives differences of 24% and the model-measurement comparison is done for SZA = 90°.

Photochemical effects on the BrO profile obtained by the SALOMON instrument from solar occultation measurements are estimated to be of 10% and are taken into account in the error estimation in accordance with the study of Ferlemann et al. (1998). Photochemical changes in the BrO slant column densities (SCD) recorded during balloon ascent are small and the DOAS BrO profile has not been corrected to 90° SZA (Ferlemann et al., 1998; Harder et al., 2000; Dorf et al., 2006b).

## 2.2 Model calculations

The REPROBUS 3D CTM has been used in a number of studies of stratospheric chemistry involving nitrogen and halogen compounds in particular through comparisons with space-borne and balloon-borne observations (e.g. Krecl et al., 2006; Berthet et al., 2005; Brohede et al., 2007). It is designed to perform annual simulations as well as detailed process studies. A description of the model is given in Lefèvre et al. (1994) and Lefèvre et al. (1998), as well as in the Appendix.

In this study, REPROBUS was integrated from 1 October 2008 to 1 October 2009 with a horizontal resolution of 2° latitude by 2° longitude. The ozone field was initialized on 1 April 2009 from the ECMWF ozone analysis. Following the work of Legras et al. (2005), REPROBUS has been driven by 3-hourly ECMWF wind fields obtained by interleaving operational analysis and forecasts. Using these more timely resolved and less noisy ECMWF wind fields reduced the ascent velocities of the upward branch of the Brewer-Dobson circulation in the tropics, largely reduced the model-measurement discrepancies by increasing the simulated global $NO_y$ and $NO_x$ amounts from increased $N_2O$ photo-oxidation (Berthet et al., 2006). In this configuration, the summer 2009 REPROBUS simulations are in agreement with the SPIRALE in situ observations (**Figure 1a**).

As sulfur chemistry is not included in REPROBUS we have conducted a simulation (hereafter called Ref-sim) constrained with typical background aerosol levels inferred from $H_2SO_4$ mixing ratios provided by the UPMC 2D model (Bekki and Pyle, 1994) and used as reference, namely without presence of volcanic aerosols. A simulation (hereafter called Sat-sim) has been set up by prescribing time-dependent variations of the stratospheric sulfate aerosol content from 1-km vertical resolution extinction measurements by the Optical Spectrograph and Infrared Imaging System (OSIRIS) instrument onboard the Odin satellite. OSIRIS aerosol extinction data used in this study are the validated version 5 retrieved at 750 nm (Bourassa et al., 2012). They compare well with the profiles inferred from the STAC balloon-borne aerosol counter (Jégou et al., 2013) thus providing confidence in the use of the data as a basis for consideration of time dependent changes of aerosol content. OSIRIS data have been averaged daily and zonally over 10° latitude bins. A standard Mie scattering model (Van de Hulst, 1957; Wiscombe, 1980; Steele and Turco, 1997) has been run to convert extinction values to $H_2SO_4$ mixing ratios from parameters of log-normal unimodal size distributions provided by the STAC instrument and used in the work of Jégou et al. (2013) in the Sarychev aerosol conditions. The derived $H_2SO_4$ mixing ratios have been then incorporated into the model over the period of presence of the Sarychev aerosols in the northern hemisphere lower stratosphere, i.e. from the beginning of July 2009 onwards. The simulation has been conducted until October 2009 because OSIRIS data at high latitudes are lacking beyond this period due to decreasing solar illumination.

We have conducted another type of simulation (hereafter called Bal-sim) consisting in adjusting the input $H_2SO_4$ mixing ratios so that the model output matches SADs observed by the STAC aerosol counter. Although similar aerosol SAD values were observed by Kravitz et al. (2011) in November 2009, i.e. ~2 months after the STAC measurements as mentioned by Jégou et al. (2013), a single vertical profile may be not representative of the geographical distribution of the still unmixed volcanic plume throughout summer 2009. To account for the range of aerosol variability as observed by STAC over the Arctic region for the August-September period (**Figure 2**) we have performed two simulations based on

the spread (1σ standard deviation) of observed SADs. We have excluded data suspected to be spoiled by balloon outgassing as deduced from joint water vapour measurements. Also, flights revealing the sporadic presence of clouds are not considered to derive the range of SADs below 12 km. Each Bal-sim simulation is respectively driven by the lower and the upper bound of observed SAD values below 20 km (**Figure 2**) from the beginning of August until the end of the model run for latitudes above 40°N. Note that in Bal-sim, $H_2SO_4$ mixing ratios in July are taken from the Sat-sim simulation.

# 3. Impact of the volcanic aerosols on stratospheric nitrogen compounds: comparisons between balloon-borne observations and model simulations

## 3.1 Photochemical conditions

$N_2O_5$ is produced mainly at night from the recombination of $NO_2$ with $NO_3$ and destroyed during the day by photolysis leading to the reformation of $NO_2$. Polar summer is characterised by continuous solar illumination preventing the formation of $N_2O_5$ (Fahey and Ravishankara, 1999) until about the beginning of August (Brühl et al., 1998), i.e. around day 213 for the considered Esrange/Kiruna location as illustrated in **Figure 3** at 17.5 km. When $NO_3$ reforms at this time, significant conversion of $NO_2$ to $N_2O_5$ occurs during the night. The associated decrease in $NO_x$ is reflected in **Figure 3**. The conversion of $N_2O_5$ to $HNO_3$ through reaction (1) occurs almost exclusively at night. As the season progresses, the increase in the conversion rate caused by the increase in night duration is moderated by the decrease in $NO_2$ amounts at the beginning of the night.

As expected, increasing SAD values in the model to reproduce the volcanic aerosol levels has no effect on $N_2O_5$ (and on the production of $HNO_3$) and on $NO_x$ during the period of continuous solar illumination. However, from the onset of $N_2O_5$ recovery a significant decrease in the $N_2O_5$ and $NO_x$ levels in comparison with the background aerosol simulation is calculated as the lifetime of $N_2O_5$ in reaction (1) is reduced (e.g. Kinnison et al., 1994) and as further nitrogen oxides are converted to the more stable $HNO_3$ reservoir.

This situation implies that the balloon flights performed from August 7, 2009 in the Kiruna region match the photochemical conditions for which volcanic aerosols likely have an impact on $NO_y$ partitioning via elevated $N_2O_5$ hydrolysis and can be suitably used to investigate heterogeneous processes.

## 3.2 $NO_2$

### 3.2.1 Model comparisons with observations

For the Sarychev situation, minima in $NO_2$ concentrations appear closely correlated with enhancements in aerosol amounts in the lower stratosphere (**Figure 4**). Thus the empirical evidence supports the view that $NO_x$ chemistry is largely driven by heterogeneous processes even in the case of a moderate volcanic eruption. The vertical structures depicted in **figure 4** confirm that the plume is not homogeneously mixed over the Arctic region ~2 months after the eruption. Minimum concentration values of 1 to 2 particles.cm$^{-3}$ (for sizes > 0.4 µm) correspond to unperturbed background extra-vortex conditions (Renard et al., 2010) and therefore indicate air masses unaffected by the volcanic aerosols. Conversely, layers with aerosol concentration increases by more than a factor of 3 (with respect to the mean profiles) can be assigned to the presence of the volcanic plume and show associated reductions in $NO_2$ by up to a factor of ~2.

**Figure 5** and **Figure 6** present the measured profiles of $NO_2$ obtained by the SPIRALE, SALOMON and DOAS instruments, together with REPROBUS model outputs for altitudes below 20 km where the Sarychev aerosols were present. In contrast to the reference simulations, the Bal-sim simulations constrained by the range of aerosol SADs observed by STAC show significant improvement in

comparison with the non-volcanic calculations with for instance average differences of 3±20% for SPIRALE-07082009. Results from the Sat-sim simulations driven by OSIRIS satellite data are very close to the Bal-sim results and are only shown for the SPIRALE flights.

It can be noted that the REPROBUS calculations do not reproduce some of the vertical structures detected by the SPIRALE instrument, i.e. between 17.5 and 19.5 km for SPIRALE-07082009 and at 17 km and 20.5 km for SPIRALE-24082009. This is likely due to the vertical resolution of the model or inaccurate simulation of mixing effects in the CTM as already mentioned in previous studies showing this kind of comparisons (e.g. Berthet et al., 2006).

Calculated differences between the volcanic-aerosol-constrained and the reference simulations provide an estimation of the chemical perturbation induced by the Sarychev aerosols. Reductions in $NO_2$ mixing ratios between 34 and 50 % are simulated on average below 19 km. For a stratosphere affected by the Pinatubo aerosols, decreases ranging from 30 to 45% have been reported both in model calculations of $NO_2$ concentrations (Kinnison et al., 1994; Webster et al., 1994) and in the $NO_2$ columns (Johnston et al., 1992; Koike et al., 1993; Koike et al., 1994; Solomon et al., 1994). At a glance, the amplitude in the $NO_2$ reduction is therefore similar for both eruptions but it should be noted that results from these above-mentioned studies were provided for different latitudes, various seasons and correspond to wider altitude ranges as a result of the larger vertical extent of the Pinatubo aerosol cloud.

### 3.2.2 One-dimensional model calculations

Some small model-measurement discrepancies in the 20-35 km altitude range as shown in the embedded plots in **Figure 5 and Figure 6** suggest that the model-measurement differences in the lower stratosphere may be only partly attributed to remaining uncertainties in calculations of transport. A way to discard a possible remaining effect of transport and improve the modelling of total $NO_y$ is to use one-dimensional (1D) calculations constrained by observations (Dufour et al., 2005; Berthet et al., 2006).

Total $NO_y$ from SPIRALE measurements can be derived from established $N_2O$-$NO_y$ correlation curves. Since the study of Michelsen et al. (1998), global emissions of $N_2O$ have increased and the $N_2O$-$NO_y$ correlations reported therein need some revision. As a consequence, we have constructed updated correlation curves from the IMK/IAA V5R_220 MIPAS-Envisat data for the high-latitude in summer stratosphere (Fischer et al., 2008; data available at http://www.imk-asf.kit.edu/english/308.php) as shown in **Figure 7** in which the Michelsen et al.'s former results are also represented for comparison. An example of the estimated vertical profile of $NO_y$ (hereafter $NO_y$*) derived from the conversion of the SPIRALE $N_2O$ profile (**Figure 1a**) using the $N_2O$-$NO_y$ ratios derived from MIPAS data is presented in **Figure 1b**. Then, following the strategy of Berthet et al. (2006) the $N_2O$ and the derived $NO_y$* profiles for SPIRALE-07082009 and SPIRALE-24082009 are used to initialise the REPROBUS 1D version.

The 1D-REPROBUS reference simulation is computed with background aerosol levels, whereas the Sarychev aerosol affected simulation is constrained with the mean observed aerosol profile presented in **Figure 2**. As a result of the $NO_y$* input in the calculations, the 1D reference simulations show very good agreement for $NO_2$ (in red in **Figure 5**) with the SPIRALE measurements above 20 km. The 1D simulations constrained by observed volcanic aerosol quantities (in yellow in **Figure 5**) match well with the in situ measurements. The calculated chemical impact on $NO_2$ gives percentage values similar to the 3D simulation results certainly because both $NO_y$* and 3D $NO_y$ profiles agree well in the lower stratosphere (**Figure 1b**). We note that fine structures in the measured profile are not reproduced by the 1D model as a matter of height resolution and interpolation (Berthet et al., 2006).

Overall the 1D $NO_y$-constrained simulations do not significantly improve the comparisons. This result confirms that the model-observations differences in the lower stratosphere can be mostly attributed to heterogeneous processes and not to spurious calculations of transport.

### 3.2.3 Saturation effect of $NO_x$ reduction

The reduction of $NO_x$ from the results described above (section 3.2.1) is significant but also indicates some saturation through reaction 1 for the range of SADs observed for the Sarychev aerosols. The partitioning between $NO_x$ and $NO_y$ is expected to become insensitive to increases in aerosol SAD beyond a certain value when $N_2O_5$ hydrolysis is the dominant sink for $NO_x$ because the night-time formation of $N_2O_5$ by reaction of $NO_2$ and $NO_3$ is quadratically dependent on $NO_x$. This effect is reflected in **Figure**

**8** presenting the $NO_2$-SAD curve constructed for the range of altitudes spanned by the volcanic plume (i.e. with different $NO_y$ amounts and photochemistry). Although the asymptotic behaviour in the $NO_2$ reduction would be more evident if shown for a given altitude level with constant SZA and varying SADs, our results indicate saturation for SAD values larger than about 4 $\mu m^2.cm^{-3}$ which is reached on average for altitudes around 18 km. The net reduction of $NO_x$ reported for the Pinatubo aerosols tends to saturate at similar SADs in the 18-22 km range, as shown in the works of Fahey et al. (1993), Kondo et al. (1997) and Sen et al. (1998).

### 3.3 $HNO_3$ and $NO_2/HNO_3$ ratio

We consider here total $HNO_3$, i.e. both in the gas phase and condensed. All the REPROBUS simulated profiles for $HNO_3$ are mostly within the errors bars of the SPIRALE measurements and only differ by less than 10% on average (not shown). Calculated amounts from Bal-sim are increased by 10-13% when including volcanic aerosols below 19 km, highlighting limited effects on $HNO_3$.

The $NO_2/HNO_3$ ratio can be used as a good approximation of the $NO_x/NO_y$ ratio to reduce the uncertainty in a model estimate of $NO_y$ (e.g. Webster et al., 1994; Berthet et al., 2006). This is especially useful for the SPIRALE flights for which modelled $NO_2$ and $HNO_3$ amounts account for more than 92% of total $NO_y$. Good agreement is obtained between the observed $NO_2/HNO_3$ ratio and the model outputs by including the Sarychev aerosols, with for instance absolute differences decreasing to 3±20% for the Bal-sim simulation for SPIRALE-07082009 (**Figure 9**). However no clear improvement can be noticed with respect to the model-measurement comparisons presented in **Figure 5** for $NO_2$ both at and above the altitudes of the plume. 1D calculations do not show improvement as well (not shown). Again this indicates that transport calculation is not a major issue in the comparisons. Reductions in the $NO_2/HNO_3$ ratios between 36 and 44% are simulated on average below 19 km for SPIRALE-07082009 and SPIRALE-24082009, respectively, when volcanic aerosols are included.

For the Pinatubo aerosol loaded stratosphere, maximum $HNO_3$ column increases of 30-40% have been measured at mid-latitudes (e.g. Koike et al., 1994). Reductions ranging from 20 to 45% have been reported both in the observed $NO_2/HNO_3$ column ratios (Koike et al., 1994) and in model calculations (Webster et al., 1994). However, quantifying the difference between both eruptions through comparisons of local concentrations versus columns remains challenging because the production efficiency of $HNO_3$ by heterogeneous processes generally depends on the altitude level where volcanic aerosols are present (Webster et al., 1994; Danilin et al., 1999). In particular, the observed signature of the Pinatubo-induced $HNO_3$ enhancement was not limited to the lower stratosphere and was prevailing above the 420-465 K (~16-18 km) vertical range (Webster et al., 1994; Santee et al., 2004).

## 4. Impact of the volcanic aerosols on the coupled catalytic cycles involving halogen, nitrogen and $HO_x$ compounds

### 4.1 Chlorine partitioning

Several studies have revealed the impact of the Pinatubo eruption on the stratospheric halogen chemistry. This has been shown to be of particular importance regarding ozone destruction processes through the partitioning of chlorine reservoir species and activation of chlorine radicals on volcanic aerosols (e.g. Solomon, 1999 and references therein).

Some volcanic eruptions are likely to inject halogenated compounds within the stratosphere therefore impacting directly the halogen content and bypassing (or adding to) in situ heterogeneous processes. For

the Sarychev volcano eruption, an injection of several ppbv of HCl in the stratosphere has been reported by Carn et al. (2016) using Microwave Limb Sounder (MLS) data, mainly below the 140 hPa level (see their Figure 4). However because of the low vertical resolution of MLS data, i.e. ~3 km, the exact altitude of injection is unclear and requires further investigation. In addition, MLS HCl measurements are known to be biased high below the 100 hPa level (Livesey et al., 2011) making difficult to infer a robust injection amount. As a consequence, the possible effect of the HCl injection on the stratospheric chlorine chemistry is not investigated in our study.

We therefore examine the direct impact of the Sarychev sulfate aerosols on the chlorine partitioning in connection with $NO_x$ and $HO_x$ in the lower stratosphere. Heterogeneous reactions on volcanic aerosols involving the $ClONO_2$ and HCl chlorine reservoirs (especially reaction 2) have been shown to play a major role in determining the abundance of active chlorine and therefore they are likely to compete with reaction 1 as a sink of $NO_x$ depending on ambient temperature values (e.g. Hanson et al., 1994). Significant decreases of HCl and corresponding increases in $ClONO_2$ have been reported for temperatures below 210 K in the lower stratosphere with a strong temperature sensitivity when volcanic aerosol amounts are large (Michelsen et al., 1999; Webster et al., 1998; Webster et al., 2000). **Table 1** presents the calculated effects of the Sarychev aerosols on the partitioning of the halogen species at 16.5 km. Simulated levels of HCl decrease by 3% (~20 pptv) which is much smaller than the change observed by Webster et al. (2000) for the Pinatubo aerosols (about -31% at 21 km). Higher levels of $ClONO_2$ are simulated post the Sarychev eruption with respect to background conditions with increases of about 16% (~20 pptv). ClO and HOCl increase by 106% (~6 pptv) and 217% (~2 pptv) respectively at daytime. It is interesting to notice that these results for ClO are comparable to the calculations of Tie et al. (1994) who show ClO increases by at least 5 pptv in the lower stratosphere for summer 1992 at a time when Pinatubo related aerosol SADs were similar to August 2009 values.

The impact of the volcanic aerosols on the chlorine partitioning appears somewhat small since it is primarily the consequence of the increasing losses of HCl by enhanced OH through reaction $HCl + OH \rightarrow Cl + H_2O$ (McElroy et al., 1992; Webster et al., 2000) rather than by reaction 2 for which the efficiency is low in the ~215-225 K range of temperatures mostly encountered in the lower stratosphere over the August-September 2009 period (see Figure 9 in Jégou et al., 2013). In fact, in the model $HO_x$ is increased by 51% (~1.4 pptv) (**Table 1**) and destruction of HCl by OH is faster than the HCl formation reaction $Cl + CH_4 \rightarrow HCl + CH_3$. An additional source of OH is due to photolysis of $HNO_3$ (Rodriguez et al., 1991; Webster et al., 2000). Also the decreased reaction rate of reaction $NO_2 + OH + M \rightarrow HNO_3 + M$ in reduced $NO_x$ conditions (Kinnison et al., 1994) may increase OH. As also described by Bekki and Pyle (1994), subsequent production of reactive chlorine and increase in ClO is accompanied by an increase in $ClONO_2$ amounts through increased rate of reaction $ClO + NO_2 + M \rightarrow ClONO_2 + M$, for which ClO is the limiting reactant. To a lesser extent, decreased rate of reaction 3 for the observed temperature range contributes to this increase. Overall, the $ClONO_2$ increase compensates for the HCl decrease in reaction 3 (Kinnison et al., 1994; Michelsen et al., 1999; Webster et al., 2000). HOCl amounts rise as a result of slightly enhanced $ClONO_2$ hydrolysis and production by enhanced $HO_x$ through reaction $HO_2 + ClO \rightarrow HOCl + O_2$.

## 4.2 Bromine compounds

### 4.2.1 Effect on BrO

Coupling between chlorine and bromine compounds is of particular importance in the lower stratosphere (e.g. Lary et al., 1996; Erle et al., 1998; Salawitch et al., 2005). Heterogeneous bromine reactions are expected to increase the coupled gas phase ClO/BrO catalytic ozone destruction cycles. Because $BrONO_2$ hydrolysis (reaction 4) is not temperature dependent, its effects on the chemistry of the lower stratosphere are primarily dependent on the aerosol loading and not on latitude or SZA (Lary et al., 1996; Kondo et al., 1997; Erle et al., 1998).

Since direct injection of bromine in the stratosphere was insignificant after the Sarychev eruption (Hormann et al., 2013) we expect that stratospheric bromine chemistry was only modified by the enhanced aerosol loading. BrO was the only key halogenated radical detected during the summer 2009 balloon campaign. Vertical profiles were provided by the SALOMON and DOAS instruments on 25

August 2009 and 7 September 2009 respectively (**Figure 10**). They were simultaneously measured with the $NO_2$ profiles presented in section 3.2. Differences between both profiles in terms of BrO amounts are mainly due to differences in SZA. When volcanic aerosol SADs are included BrO amounts are increased in the lower stratosphere, matching the observations within the error bars (**Figure 10**).

Simulated results related to the bromine chemistry at 16.5 km are presented in **Table 1** for the August-September 2009 period. At daytime part of the BrO enhancement is linked to the decreased loss by the three body reaction with decreased $NO_2$. The other part is expected to be controlled by $BrONO_2$ hydrolysis which is by far the most efficient bromine heterogeneous reaction in the temperature range observed in our study (Hanson and Ravishankara, 1995; Hanson et al., 1996). Under high aerosol loading the rate of the $BrONO_2$ hydrolysis is likely to compete with the $BrONO_2$ photolysis and with other gas phase reactions which normally control the bromine partitioning at daytime (Lary et al., 1996). Here note that the conclusion of Kreycy et al., (2013) on a possibly larger ratio of the photolysis and the three body formation reaction for $BrONO_2$ ($J(BrONO_2)/k_{BrO+NO_2}$) than compiled by Sander et al. (2011) is not affected by the presence of the Sarychev aerosols in the lower stratosphere, since they have addressed observations with SZA <92.5° at 31 km (i.e., tangent heights >24 km). After sunset $BrONO_2$ production is ceasing and its enhanced hydrolysis on volcanic aerosols leads to strongly increased formation of HOBr (+3.9 pptv or +141%) at an early stage of the night so that little $BrONO_2$ remains before dawn. This conversion at night-time results in further release of OH and Br atoms in the morning through photolysis of HOBr.

However, it is not clear if $BrONO_2$ hydrolysis is mainly responsible for the increase in BrO within the lowermost stratosphere. Dedicated simulations to estimate the respective contribution of gas-phase chemistry and heterogeneous processes on the control of BrO production under volcanic conditions have thus been performed. The effects of the Sarychev aerosols on each chemical compound are calculated by switching off reaction 4 and compared in terms of percentage differences with the simulations including all chemistry. Results are summarized in **Table 1**. It particularly shows that under the Sarychev aerosol loading, only 16% of the 22% (0.9 pptv) increase in daytime BrO at 16.5 km for the August-September 2009 period is produced from $BrONO_2$ hydrolysis. This result implies that bromine chemistry in the gas phase coupled to processes controlling the $NO_y$ partitioning mainly govern BrO amounts (e.g., Lary et al., 1996).

### 4.2.2 Role of $BrONO_2$ hydrolysis on other compounds

As shown in **Table 1** for an altitude of 16.5 km, at night $BrONO_2$ amounts are mainly affected by reaction 4 which controls 98% of its decrease under volcanic aerosol influence. Nearly 100% of the night-time HOBr production is due to $BrONO_2$ hydrolysis which accounts for 44% of the increase in OH radical amounts from the subsequent photolysis of HOBr at dawn. Therefore, under volcanic conditions enhanced $BrONO_2$ hydrolysis nearly matches the contribution of nitrogen chemistry (see section 4.1) as a source of OH (e.g., Hanisco et al., 2001).

This additional release of OH radicals has significant consequences in the chemistry of the lower stratosphere. In our study the reduction in $NO_x$ from $BrONO_2$ hydrolysis are small (less than 2%) as well as the overall effects on nitrogen partitioning confirming the conclusions of Lary et al. (1996) and Kondo et al. (1997). In contrast, there is substantial repartitioning of the active chlorine family species. The catalytic increase in OH due to the hydrolysis of $BrONO_2$ leads to a reduction in the HCl lifetime which is primarily dependent on the aerosol loading (Tie and Brasseur, 1996). The additionally produced OH converts further HCl to ClO and, ultimately, to $ClONO_2$. As shown in **Table 1**, ~60% of the HCl decrease, 39% of the ClO increase and 66% of the $ClONO_2$ increase are due to reaction 4 under the Sarychev aerosol loading, thus illustrating a significant enhancement of the coupling between the stratospheric chlorine and bromine photo-chemistry.

# 5. Stratospheric ozone

## 5.1 Chemical ozone change

It is interesting to estimate the stratospheric ozone depletion induced by the Sarychev eruption. As said above, the model does not directly calculate possible effects of aerosols on stratospheric temperature and circulation. All our simulations use the same transport calculations, whereas ozone loss from Pinatubo in the northern mid-latitudes can be both attributed to chemical and transport (such as increased tropical upwelling) effects (e.g. Telford et al., 2009; Dhomse et al., 2015). In the following, we therefore solely calculate the change in ozone due to photochemistry.

We then compare model simulations with enhanced and background aerosol levels (**Figure 11**). Results indicate chemical reductions in ozone of a few percent following the eruption when aerosol levels are computed from the OSIRIS space-borne data. Accumulated ozone depletion reaches its maximum above Kiruna near 16 km from around mid-September with changes of -22 ppbv corresponding to -1.5%. Below this level changes range from -10 ppbv to -18 ppbv, i.e. -2.5% to -3.5%. From the upper bound of the Bal-sim outputs calculated ozone depletion reaches -25 ppbv (-2.8%) and -35 ppbv (-4%) at 16.5 km and 14 km, respectively (not shown).

We note that for the post-Pinatubo eruption period, ozone reductions as large as -30% were measured for the 12 and 22 km altitude range monitored at some mid-latitude locations in winter and spring (Hofmann et al., 1994) but these losses are both due dynamical and chemical perturbations. Through 2D modelling, ozone losses of up to -20% directly resulting from heterogeneous chemical processes were calculated in the northern hemisphere lower stratosphere over the first year following the Pinatubo eruption (Pitari and Rizi, 1993; Tie et al., 1994). The calculated chemical loss had reduced to values much closer to those simulated for the Sarychev aerosols, i.e. ~-5%, at 60°N in the autumn 1992 extra-polar vortex conditions (Tie et al., 1994).

## 5.2 Chemical mechanisms for the ozone change in the lower stratosphere

In the lower stratosphere ozone removal rates are mainly controlled by the $HO_x$ and halogen catalytic cycles which have been found to typically account for 30-50% and 30% of the total ozone loss respectively, in non-volcanic conditions (Portmann et al., 1999; Salawitch et al., 2005). The $NO_x$ cycles play a relatively minor role in the direct removal of ozone in the lower stratosphere but, as a result of the coupling among the $NO_x$, $HO_x$ and halogen cycles, the rate of ozone removal is still very sensitive to the concentration of $NO_x$ (Wennberg et al., 1994; Gao et al., 1999; Portmann et al., 1999; Salawitch et al., 2005). Through the reaction of $HO_2$ with NO ($HO_2 + NO \rightarrow NO_2 + OH$), the decreased $NO_x$ concentrations after the Sarychev eruption result in a larger $HO_2$/OH ratio (as shown in **Table 1**) than for background conditions ($HO_2$/OH ratios typically ranging from 4 to 7). Because the photochemical removal of ozone in the lower stratosphere is dominated by processes involving $HO_2$, catalytic ozone destruction by $HO_x$ cycles is likely to be amplified after volcanic eruptions (Wennberg et al., 1994; 1995) though ozone loss rates are limited due to the saturation of the $NO_x/NO_y$ response. After the eruption of Sarychev the effectiveness of halogen cycles is enhanced due to increased $ClO_x$ resulting from OH increase (**Table 1**) (as explained in section 4.1). However, as said above heterogeneous reactions activating chlorine are strongly and non-linearly dependent on temperature, implying slow rates at the average mid-latitude temperature conditions (minimum values of 215 K) (Hanson et al., 1994; Webster et al., 1998; Michelsen et al., 1999). Under these conditions the simulated depletion in ozone is restrained similarly to the finding of Tie et al. (1994) for the post-Pinatubo eruption period.

Part of the ozone depletion can be related to the coupled $BrO_x/ClO_x$ cycle which is expected to be responsible for 20-25% of the halogen-controlled loss under non-volcanic aerosol conditions (Portmann et al., 1999; Salawitch et al., 2005). **Table 1** shows that the hydrolysis of $BrONO_2$ accounts for more than 22% of the ozone loss at 16.5 km after the Sarychev eruption. As described in section 4.2.2, this is due to reaction 4 acting as a source of OH, reducing the HCl lifetime and thereby indirectly amplifying the chlorine-mediated ozone depletion. Because the sticking coefficient for hydrolysis of $BrONO_2$ on

sulfate aerosols is not temperature dependent, this effect occurs at all latitudes and seasons in the lower stratosphere during high aerosol loading periods (Lary et al., 1996; Tie and Brasseur, 1996).

## 6. Summary and conclusions

Our study provides key observations of the chemical perturbation in the lower stratosphere by the moderate Sarychev volcano eruption in June 2009. 3D and 1D CTM simulations are performed to interpret balloon-borne observations of some key chemical species made in the summer high-latitude lower stratosphere. The modelled chemical response to the volcanic aerosols is treated by comparing simulations using background aerosol levels and simulations driven by volcanic aerosol amounts inferred from balloon-borne and space-borne observations.

Quantifying the impact of volcanic aerosols on stratospheric ozone chemistry is difficult as chemical and dynamical (radiative) effects simultaneously occur (Pitari and Rizi, 1993; Robock, 2000; Al-Saadi et al., 2001; Aquila et al., 2013). The model is a CTM driven by ECMWF off-line meteorological data and does not describe radiative processes. In other words, volcanic aerosol radiative effects are not directly interactive with the circulation computed by the model. Radiative processes from the injection of volcanic aerosols in the tropics have been shown to have an impact on mean meridional circulation and ozone transport (Brasseur and Granier, 1992; Pitari et Rizi, 1993). In our study, effects of the Sarychev aerosols on mid-latitude stratospheric dynamics, if any, are at least at the first order intrinsically taken into account in the ECMWF analyses used for all simulations. REPROBUS does not take into account the aerosol impact on calculated photolysis rates which is likely to result in some differences between models when this process is computed or ignored (Pitari et Rizi, 1993; Pitari et al., 2014). However because the Sarychev eruption has impacted only the lower stratosphere at mid- and high latitudes the effect on the photolysis frequency of molecular oxygen and ozone due to absorption and backscattering of solar radiation by the volcanic aerosols is expected to be very small in these regions (Tie et al., 1994). Therefore, since all our simulations have been driven with the same wind and temperature fields our approach only estimates the chemical effects of the Sarychev aerosols.

The $NO_y$ chemistry appears to be very sensitive to the increase in SAD within the lower stratosphere resulting from the Sarychev eruption. A decrease in the $NO_x$ abundances is evident but shows some saturation as emphasized in a number of studies referring to cases of high sulfate aerosol loadings (e.g. Fahey et al., 1993). The effect of volcanic aerosols on nitrogen partitioning is also reflected in the calculated production of $HNO_3$ as a result of the decrease of the $N_2O_5$ nitrogen reservoir from its enhanced hydrolysis and $NO_x$ reduction.

Although direct comparisons in terms of solar illumination, latitude, injection altitudes and temperature are not possible for distinct volcanic eruptions such as Pinatubo and Sarychev, it is interesting to compare the effect of both eruptions on the photochemistry of the lower stratosphere. Overall, although different in magnitude, the eruptions of Pinatubo and Sarychev show similar observed and simulated depletion of $NO_2$, probably due to the saturation effect of the enhanced $N_2O_5$ hydrolysis. In comparison with the Pinatubo period, the Sarychev aerosols led to less overall $HNO_3$ production in the stratosphere possibly because the related $HNO_3$ enhancement has been shown to be considerably weaker in the lowermost stratosphere (below ~18 km) than for sulfur injection into higher altitudes (Webster et al., 1994; Santee et al., 2004). However, one must notice that previously reported modelling studies on the Pinatubo aerosols were conducted with former chemical kinetic rate constants and photolysis rates which have been largely updated ever since, somewhat adding complexity for comparisons discussed within the present study.

For the Pinatubo aerosols, ozone destruction was not observed throughout the volcanic aerosol layer because $N_2O_5$ hydrolysis reduced $NO_x$ related ozone loss, which even resulted in small increases of ozone in the middle stratosphere (Bekki and Pyle, 1994; Tie and Brasseur, 1995). For the Sarychev eruption, the volcanic aerosol layer is restrained to altitude levels below 19 km where the ozone destruction processes by $HO_x$ and halogen catalytic cycles are expected to play a major role (e.g.

Salawitch et al., 2005) with some sensitivity towards $NO_x$ levels. To summarize, the increased production of $HNO_3$ via $N_2O_5$ hydrolysis enhances the photolytic production of OH from $HNO_3$. As a result, the gas-phase sink for HCl by reaction with OH is slightly enhanced and is associated with an increase of ClO amounts. An important result from the heterogeneous hydrolysis of $BrONO_2$ is the formation and subsequent photolysis of additional HOBr. The OH so produced additionally converts HCl to ClO (and ultimately to $ClONO_2$). Accordingly, there is substantial repartitioning of the active chlorine but effects of the $BrONO_2$ hydrolysis on nitrogen partitioning are insignificant. In this chemical context, the magnitude of the ozone response to the Sarychev volcanic perturbation appears restricted (for instance -22 ppbv or -1.5% around 16 km) because the saturation of the $NO_x/NO_y$ response limits the increase in $HO_x$ and in active chlorine (ClO) by enhanced $HO_x$, precluding important ozone loss rates. Moreover, stratospheric temperatures remained too high (i.e. mainly above 215 K) for efficient heterogeneous conversion of $ClONO_2$ to active chlorine, which could have led to significant ozone depletion. For these temperature conditions, reaction 2 is not expected to compete with $N_2O_5$ hydrolysis in the $NO_y$ partitioning (Fahey et al., 1993; Cox et al., 1994).

However limitations in our model simulations also contribute to some model-measurement discrepancies. A first major difficulty is to drive the model simulations with representative and consistent inputs in term of volcanic aerosol loading. To address this issue, two different model runs for aerosol forcing have been performed, one using OSIRIS satellite data converted to aerosol SAD fields and the other one from in situ balloon-borne observations. The OSIRIS satellite data represent zonally and daily averaged values of SAD which may vary from a 3D construction based on the local surface areas. The possible presence of aerosol streamers (geographical variations of the aerosol content) resulting from the transport of the volcanic aerosols over the northern hemisphere present from mid-July to September 2009 is likely to affect locally and regionally the $N_2O_5$ abundances and, to a lesser extent, $NO_2$ and $HNO_3$ (Jucks et al. 1999; Küll et al., 2002). If our aerosol SAD dataset had been obtained when the local concentrations were higher than the zonal mean values, then the calculated rate of the heterogeneous reactions would be biased low and calculated $NO_x$ and $HNO_3$ abundances would be systematically biased high and low respectively. This is not however evident in all our comparisons from simulations based on OSIRIS aerosols. The second type of aerosol-constrained simulation uses SADs from balloon-borne observed profiles. By definition, such in situ observations deal with a particular location. Extrapolating in situ derived SADs to drive a 3D model at a large scale may induce inaccurate simulations of the chemical impact of the aerosols (Kondo et al., 2000). To account for this SAD-related uncertainty, our simulations based on in situ data encompass the range of SADs derived from the STAC balloon-borne observations over the August-September 2009 period. Both satellite- and balloon-driven simulations give similar results in terms of $NO_2$ and $HNO_3$ amounts possibly because the in situ observations represent well the aerosol loading at the northern mid-latitudes. Another explanation is that the saturation effect (roughly when SADs become larger than 3 $\mu m^2.cm^{-3}$) of the $NO_x/NO_y$ ratio is more relevant for the range of observed SADs than spatiotemporal inhomogeneities.

Secondly, adequate modelling of transport is also crucial for the partitioning of $NO_y$. Processes that control the vertical profiles of $NO_2$ and $HNO_3$ in the stratosphere are based on a complex interplay between dynamics and chemistry with the key issue to accurately simulate total $NO_y$ which may be not systematically achieved with 3D CTM calculations. Improved simulations of transport can be obtained by combing operational analyses with forecasts to construct 3-hourly meteorological data to drive the CTM (Berthet et al., 2006). We have applied this strategy in the present study. Using 1D modelling driven by in situ observations or calculating $NO_2/HNO_3$ ratios to reduce transport effects does not clearly improve the model-measurement comparisons for the lower stratosphere. Although some features in the vertical profiles are not systematically captured by the model, this tends to indicate that the error in calculated transport is not large enough to account for the overall difference between measured and modelled $NO_2$ and $HNO_3$ when no volcanic aerosol loading is included in the model. Rather, these results show some evidence of the role of heterogeneous reactions at the surface of volcanic aerosols.

Thirdly, part of the discrepancies between model and observations might be attributed to spatial resolution issues. It may be tricky to compare model calculations with high resolution in situ profiles and with remote sensing observations integrating over tens of kilometres (Berthet et al., 2007). For instance, discrepancies between remote sensing observations and model calculations have been reported for stratospheric $NO_3$ in case of localized temperature inhomogeneities as a result of the strong dependence of $NO_3$ cross sections and kinetics on temperature (Renard et al., 2001). $N_2O_5$ and $NO_2$ may

be subsequently impacted because $NO_3$, together with $NO_2$, plays a central role in the equilibrium reaction controlling $N_2O_5$ in the gas phase.

In our study, no comprehensive sulfur chemistry is included in the model. We have also excluded dynamical and radiative effects on the ozone response which have been shown to be of primary importance when dense volcanic clouds are present (e.g. Pitari and Rizi, 1993; Kinnison et al., 1994; Tie et al., 1994; Al-Saadi et al., 2001). In a forthcoming study it would be interesting to compare dynamical/radiative and chemical effects of moderate volcanic eruptions on stratospheric ozone using Chemistry-Climate models with full sulfur chemistry and aerosol-dynamics interactive calculations.

Finally, it might be interesting to investigate the effects of other volcanic plumes coming from moderate volcanic eruptions which are then transported to high-latitude regions when stratospheric temperatures are more favourable for chlorine activation and enhanced ozone loss (e.g. in winter). Activation of chlorine from volcanic sulfate aerosols and associated ozone depletion is arguably more significant in the cold temperature conditions of winter/spring, even above the formation threshold of Polar Stratospheric Clouds (Hanson et al., 1994). The eruption of the Calbuco volcano in the southern hemisphere in April 2015 could be a good candidate for the study of this process (Solomon et al., 2016).

**Acknowledgements.**

The authors are grateful to the CNES (French acronym for "Centre National d'Etudes Spatiales") balloon launching team for successful operations and the Swedish Space Corporation at Esrange. The STRAPOLETE project and the associated balloon campaign has been funded by the French "Agence Nationale de la Recherche" (ANR-BLAN08-1-31627), CNES, and the "Institut Polaire Paul-Emile Victor" (IPEV). The study is supported by the French Labex « Étude des géofluides et des VOLatils– Terre, Atmosphère et Interfaces - Ressources et Environnement (VOLTAIRE) (ANR-10-LABX-100-01) managed by the University of Orleans. The ETHER database (CNES-INSU/CNRS) is partner of the project. Further support for the DOAS balloon measurements came through the Deutsche Forschungsgemeinschaft, DFG (grants PF-384/5-1 and 384/5-1 and PF384/9-1/2), and the European projects EU projects Reconcile (FP7-ENV-2008-1-226365) and SHIVA (FP7-ENV-2007-1-226224). We thank Michel Van Roozendael and Caroline Fayt from BIRA/IASB in Belgium for making available the WINDOAS algorithm very well-adapted for data reduction methods based on the Differential Optical Absorption Technique. We acknowledge the MIPAS/Envisat team from Karlsruhe Institute of Technology (KIT) for making IMK/IAA data available.

## Appendix A: Technical description

### A.1 The STAC aerosol counter

Aerosol size distributions are provided in the 0.4–5 μm diameter size range (Ovarlez and Ovarlez, 1995; Renard et al., 2008). Since 2008, the number of available size classes has been increased from 7 to 14 within this size range (Renard et al., 2010). The counting uncertainty is obtained from the statistical probability given by Poisson counting statistics (Willeke and Liu, 1976). This uncertainty, defined as the relative standard deviation, is 60% for aerosol concentrations of $10^{-3}$ $cm^{-3}$, 20% for $10^{-2}$ $cm^{-3}$, and 6% for concentrations higher than $10^{-1}$ $cm^{-3}$. Laboratory comparisons between two copies of the STAC aerosol counter using identical aerosol samples have shown differences of ±10% for concentrations higher than $10^{-2}$ $cm^{-3}$. From these results, we define a measurement precision limited to ±10%. It should be noted that comparisons with the aerosol concentrations measured by the University of Wyoming optical particle counter (Deshler et al., 2003) have shown consistent results between both instruments (Renard et al., 2002). STAC is calibrated in order to provide size distributions of non-absorbing liquid aerosols which have been unambiguously observed in the 8–19 km altitude range in the case of the Sarychev eruption (Jégou et al., 2013). Aerosol distribution moments are derived using well-known analytical expressions. Using a statistical approach as described in Deshler et al. (2003), STAC counting precision (Poisson statistics and the ±10% measurement reproducibility) translate into uncertainties on distribution moments, with estimated values of 40% for SAD. Profiles are typically averaged over a vertical range of 250 m (corresponding to ~1 minute of measurements).

### A.2 The SPIRALE in situ infrared spectrometer

A detailed description of the instrumental characteristics of SPIRALE and of its operating mode can be found in Moreau et al. (2005). Six tunable laser diodes emitting in spectral micro-windows (< 1 $cm^{-1}$) in the mid-infrared domain (1250 to 3000 $cm^{-1}$) are used for in situ measurements of trace gas species from the upper troposphere to the stratosphere. The six laser beams are injected into a multipass Heriott cell, comprising two mirrors spaced 3.50 m apart by a telescopic mast, allowing for 434.0 m optical path. This cell is deployed under the gondola during the flight, above ~9 km altitude, i.e. when pressure is below ~300 hPa and thus absorption lines are significantly narrower than the scanned micro-windows. Species concentrations are retrieved from direct absorption, by fitting experimental spectra with spectra calculated using HITRAN 2012 database (Rothman et al., 2013) and the temperature and pressure measured on board the gondola. Measurements of pressure (by two calibrated and temperature-regulated capacitance manometers) and temperature (by two probes made of resistive platinum wire) allow for conversion of the species concentrations to volume mixing ratios. Uncertainties on these parameters are negligible regarding the other uncertainties discussed below. The instrument provides measurements each 1.1 s, thus with a vertical resolution of a few meters depending on the vertical velocity of the balloon (2 to 5 m $s^{-1}$). Absorption lines in the micro-windows 1260.95-1261.25 $cm^{-1}$, 1598.45-1598.85 $cm^{-1}$ and 1701.50-1701.80 $cm^{-1}$ were selected for $N_2O$, $NO_2$ and $HNO_3$, respectively. The total error for the volume mixing ratios has been assessed by taking into account the random errors and the systematic errors, and combining them as the square root of their quadratic sum (Moreau et al., 2005). There are two important sources of random errors: (1) the fluctuations of the laser background emission signal and (2) the signal-to-noise ratio. These error sources are the main contributions for $NO_2$ giving a total uncertainty of 30% at the lower altitudes (around 15 km), gradually reduced to 20% around 20 km, and decreasing to 5% at higher altitudes (above 30 km). For $HNO_3$ these random errors are less significant but two sources of systematic errors have to be considered: the laser line width (an intrinsic characteristic of the laser diode) and the non-linearity of the detectors resulting in an uncertainty of 20% on the whole profile. Concerning $N_2O$ and ozone, which are abundant and measured using detection systems with proper linearity of the photovoltaic conversion, the overall uncertainties are 3% over the whole vertical profile, and decrease from 10% at 14 km (i.e. for mixing ratios below 1 ppmv) to 5% above 17 km, respectively. With respect to the above errors, systematic errors on spectroscopic data (essentially molecular line strength and pressure broadening coefficients) are considered to be negligible for these well studied species (Rothman et al., 2013). SPIRALE has been used routinely during the 2000's, in

particular as part of European projects and satellite validation campaigns (Grossel et al., 2010; Mébarki et al., 2010; Krysztofiak et al., 2012 and 2015, and references therein).

### A.3 The DOAS remote-sensing UV-visible spectrometer

Direct solar spectra from two UV/visible DOAS spectrometers are collected onboard the azimuth-controlled LPMA/DOAS (Limb Profile Monitor of the Atmosphere/Differential Optical Absorption Spectroscopy) balloon payload which carries a sun-tracker (Hawat et al., 1995). The solar reference spectrum is usually the spectrum for which the air mass along the line-of-sight and the residual trace gas absorption are minimal. The residual absorption in the solar reference is determined using Langley's extrapolation to zero air mass. Rayleigh and Mie scattering are accounted for by including a third order polynomial in the fitting procedure. The relative wavelength alignment of the absorption cross sections and the solar reference spectrum is fixed and only the measured spectrum is allowed to shift and stretch. $O_3$ Slant Column Densities (SCDs) are retrieved from the differential structures in the Chappuis absorption band between 545 nm and 615 nm. The line-of-sight absorptions of $NO_2$ are inferred from the 435 nm to 485 nm wavelength range. Two $O_3$ absorption cross sections recorded in the laboratory at 230K and 244 K, aligned to cross sections from Voigt et al. (2001), are orthogonalized and fitted simultaneously. Broad band spectral features are represented by a fourth order polynomial. Additional complications arise from the temperature dependence of the $NO_2$ absorption cross section (Pfeilsticker et al., 1999). The $NO_2$ analysis is performed using absorption cross sections recorded in the laboratory, scaled and aligned to convolved and orthogonalized cross sections from Harder et al. (1997) taken at 217 K, and 230 K. The error bars of the retrieved SCDs are estimated via Gaussian error propagation mainly from the statistical error given by the fitting routine, the error in determining the residual absorber amount in the solar reference spectrum and the errors of the absorption cross sections. In total, typical accuracies of the DOAS $O_3$ and $NO_2$ measurements are better than 5% and 10%, respectively. The retrieval process for $NO_2$ is described in Butz et al. (2006).

Bromine monoxide (BrO) is detected in the UV wavelength range from 346 nm to 360 nm as recommended by Aliwell et al. (2002). This wavelength range contains the UV vibration absorption bands (4−0 at 354.7 nm, and 5−0 at 348.8 nm) of the $A(^2\pi) \leftarrow X(^2\pi)$ electronic transition of BrO. Typical optical densities are $10^{-4}$−$10^{-3}$ for UV vibration absorption bands. The set of reference spectra used contains a $NO_2$ reference spectrum for T=233 K, and two $O_3$ spectra at T=197 K and T=253 K, in order to account for temperature effects. All $NO_2$ and $O_3$ spectra were recorded with the balloon spectrograph in the laboratory. The BrO reference is the absolute cross-section measured by Wahner et al. (1988), with the wavelength calibration taken from our own laboratory measurements. Profile information was obtained by a least-squares profile inversion technique (Maximum A Posteriori) (Rodgers, 2000). Further details on the BrO DOAS-retrieval and the profile inversion can be found in Harder et al. (1998) and (2000), Aliwell et al. (2002), Dorf et al. (2006b) and Kreycy et al. (2013).

### A.4 The SALOMON remote-sensing UV-visible spectrometer

The data presented in this study were obtained using a SAOZ-type UV-visible spectrometer (Pommereau and Piquard, 1994) connected to a sun/moon tracker for the detection of ozone and $NO_2$ amounts. The one-band spectral window of SALOMON between 400 and 950 nm is adequate for the retrieval of absorption features over large spectral ranges, i.e. roughly from 400 to 680 nm for ozone and from 400 to 550 nm for $NO_2$. The spectrum recorded at float altitude (more than 36.5 km) corresponds to a minimum air mass and is considered as a reference spectrum. Occultation spectra recorded for elevation angles between 0° and -5° below the gondola horizon are taken into account for the retrieval of the SCDs. Owing to the thermal insulation of the spectrometer, no spectral drift of the Fraunhofer lines and no instrumental resolution changes have been observed between the reference and the occultation spectra. The Rayleigh scattering contribution is calculated and removed from the spectra using these profiles and the spectral cross-sections given by Bucholtz (1995). Then, $O_3$ and $NO_2$ SCDs are determined by least-squares fits using the University of Bremen high resolution absorption cross-sections convolved to the spectral resolution of the instrument (data available from http://www.iup.uni-bremen.de/gruppen/molspec/databases/index.html). Aerosols are a major low frequency spectral contribution which is removed by a high-pass filter to derive the $NO_2$ SCDs. All lines of sight are not

used to derive SCDs since the retrieval is performed only when signal-to-noise ratios (computed in our case by the ratio of the fit maximum amplitude to the standard deviation between the measurement and the fit) are greater than 1. $NO_2$ fitting errors are typically of 5-9% for SCDs crossing the altitude levels of the volcanic aerosol layer (i.e. below ~19 km). Vertical concentration profiles have been derived using an a posteriori least-squares inversion technique (Rodgers et al., 2000) taking into account the fitting error and the uncertainties of the cross sections. Note that the data reduction method used in this study is described by Renard et al. (2000) and Berthet et al. (2002).

For the flight presented in this study we have added a HR4000 UV spectrometer from Ocean Optics to detect BrO absorption lines in the 346-360 nm range as done for the DOAS instrument. The spectrometer is thermally insulated and regulated using Peltier devices to avoid spectral shifts. It has its own connection to the sun tracker but collects the sunlight simultaneously with a Jobin-Yvon UV-visible spectrometer. We use the same data reduction method as for DOAS as described in details by Dorf et al. (2006b) to retrieve SCDs and the vertical profile of BrO. In our case the Wahner et al. BrO and Bremen ozone and $NO_2$ cross sections are convolved to the resolution of the instrument determined in the laboratory using a UV lamp. SCD data are smoothed to increase the signal-to-noise ratio. The altitude grid for profile inversion is 2 km. Associated random errors are those provided by the spectral fit. The major systematic error comes from the uncertain estimation of the residual BrO column above float altitude.

## Appendix B: Model description

The REPROBUS 3D CTM computes the evolution of 55 species by means of about 160 photolytic gas-phase and heterogeneous reactions, with a time step of 15 minutes in this study. A semi-Lagrangian code transports 40 species or chemical families, typically long-lived tracers but also more unstable compounds (Lefèvre et al., 1994; Lefèvre et al., 1998).

Temperature, winds and surface pressure are specified from the 3D European Centre for Medium-Range Weather Forecast (ECMWF) meteorological data from the surface up to 0.01 hPa (i.e. about 80 km in altitude) on 91 levels. This results in a vertical resolution of about 0.45 km in the lower stratosphere. REPROBUS is driven by 3-hourly ECMWF wind fields obtained by interleaving operational analysis and forecasts because in this way spurious calculation of transport is reduced in comparison with simulations based on 6-hourly analysis (Legras et al., 2005; Berthet et al., 2006).

Gas-phase kinetics parameters used in the present study are based on the recommendation by the Jet-Propulsion-Laboratory (JPL) described in Sander et al. (2011). In particular for nitrogen gas-phase chemistry, revised kinetic data were recommended because, following a number of studies (e.g. Brown et al., 1999; Gao et al., 1999; Jucks et al., 1999; Osterman et al., 1999; Kondo et al., 2000; Prasad, 2003), a lower rate for the reaction of $NO_2$ with OH and a higher rate for $HNO_3$ with OH significantly reduced model-measurement discrepancies highlighted in former published work (e.g. Fahey et al., 1993; Kondo et al., 1997; Sen et al., 1998).

The heterogeneous chemistry module includes reactions on liquid aerosols. An analytical expression is used to calculate the equilibrium composition and volume of the $H_2SO_4$-$H_2O$ droplets as a function of temperature and the total amounts of $H_2O$ and $H_2SO_4$ (Carslaw et al., 1995). The routine calculates the aqueous phase concentrations for the soluble species HCl, HBr, HOCl, and HOBr to calculate the rates of the heterogeneous reactions involving these compounds on stratospheric liquid aerosols. Reactions of $N_2O_5$, $ClONO_2$, and $BrONO_2$ on/in sulfuric acid are usually dependent on the species' Henry's law solubility and liquid phase diffusion coefficient in the liquid as well as the surface and/or liquid phase reaction rates (Hanson et al., 1994; Shi et al., 2001; Sander et al., 2011). $N_2O_5$ hydrolysis takes place at the surface of the particles (Hanson et al., 1994). As in a number of previous studies (e.g. Mills et al., 1993; Gao et al., 1999; Bracher et al., 2005) REPROBUS computes a $\gamma$ reaction efficiency of 0.1 as default value (0.05-0.2 in Sander et al., 2011) and which is independent of temperature and acid composition. The reaction rate is proportional to $\gamma$ and increases with aerosol SAD. For heterogeneous reactions involving $ClONO_2$, kinetics are taken from the well-detailed uptake model of Shi et al. (2001) which uses the parameterization of $H_2SO_4/H_2O$ composition of Tabazadeh et al. (1997). These processes are strong functions of the acid composition and temperature. Note that the $\gamma$ reaction efficiency for

$ClONO_2$ described in the JPL recommendation of Sander et al. (2011) is taken from Shi et al. (2001). The $BrONO_2$ reactivity on sulfuric acid particles is computed from the JPL parameterization which is based on the work of Hanson (2003) and shows a rather limited dependence on acid composition and temperature.

Initialized amounts of species are taken from a long-term simulation from the UPMC 2D model (Bekki and Pyle, 1994; Weisenstein and Bekki; 2006). Initialization of stratospheric chlorine precursors is based on scenarios defined by the World Meteorological Organization (WMO, 2014). Total inorganic chlorine ($Cl_y$ = HCl + $ClONO_2$ + HOCl + ClO + $Cl_2O_2$) is calculated by the model, and approaches 3.3 ppbv in the upper stratosphere in 2009, in accordance with the WMO (2014). Note that as expected this value is reduced compared to the study (3.7 ppbv) by Berthet et al. (2005). Total stratospheric inorganic bromine takes into account the contributions from Halons, methyl bromide and very-short-lived bromine compounds to reach 19.5 pptv, matching the scenario given by WMO (2010) updated from Dorf et al. (2006a).

Gaseous sulfur chemistry is not included in the REPROBUS CTM. The UPMC 2D model climatology (Bekki and Pyle, 1994) provides the initialization of $H_2SO_4$ mixing ratios for the background aerosols. Liquid particles are formed in equilibrium and are assumed to have a predefined number density. Mean particle radii and SADs of the liquid aerosols are calculated from the number density and the amount of $H_2SO_4$ and $H_2O$ assuming a lognormal unimodal distribution with a fixed distribution width.

## References:


Al-Saadi, J., Pierce, R., Fairlie, T., Kleb, M., Eckman, R., Grose, W., Natarajan, M., and Olson, J.: Response of middle atmosphere chemistry and dynamics to volcanically elevated sulfate aerosol: Three-dimensional coupled model simulations, J. Geophys. Res., 106, 27255–27275, 2001.

Aliwell, S., Van Roozendael, M., Johnston, P., Richter, A., Wagner, T., Arlander, D., Burrows, J., Fish, D., Jones, R., Tornkvist, K., Lambert, J.-C., Pfeilsticker, K., and Pundt, I.: Analysis for BrO in zenith-sky spectra: An intercomparison exercise for analysis improvement, J. Geophys. Res., 107, doi:10.1029/2001JD000329, 4199 pp., 2002.

Aquila, V., Oman, L. D., Stolarski, R., Douglass, A. R., and Newman, P. A.: The response of ozone and nitrogen dioxide to the eruption of Mt. Pinatubo at southern and northern midlatitudes, J. Atmos. Sci., 70, 894–900, 2013.

Bekki S. and Pyle J. A.: A two-dimensional study of the volcanic eruption of Mount Pinatubo, Geophys. Res. Lett., 99, D9, 18,861-18,869, 1994.

Berthet, G., Renard, J.-B., Brogniez, C., Robert, C., Chartier, M., and Pirre, M., Optical and physical properties of stratospheric aerosols from balloon measurements in the visible and near-infrared domain: 1. Analysis of aerosol extinction spectra from the AMON and SALOMON instruments, Appl. Opt., 41(36), 7522-7539, 2002.

Berthet, G., Ricaud, P., Lefèvre, F., Le Flochmoën, E., Urban, J., Barret, B., Lautié, N., Dupuy, E., De La Noë, J., and Murtagh, D.: Nighttime chlorine monoxide observations by the Odin satellite and implications on the $Cl_2O_2$/ClO equilibrium, Geophys. Res. Lett., doi:10.1029/2005GL022649, 32, L11812, 2005.

Berthet, G., Huret, N., Lefèvre, F., Moreau, G., Robert, C., Chartier, M., Catoire, V., Barret, B., Pisso, I., and Pomathiod, L.: On the ability of chemical transport models to simulate the vertical structure of the $N_2O$, $NO_2$ and $HNO_3$ species in the mid-latitude stratosphere, Atmos. Chem. Phys., 6, 1599-1609, 2006.

Berthet, G, Renard, J.-B., Catoire, V., Chartier, M., Robert, C., Huret, N., Coquelet, F., Bourgeois, Q., Rivière, E. D., Barret, B., Lefèvre, F., and Hauchecorne, A.: Remote sensing measurements in the polar vortex: comparison to in situ observations and implications for the simultaneous retrievals and analysis of the $NO_2$ and OClO species, J. Geophys. Res., 112, D21310, doi:10.1029/2007JD008699, 2007.

Borrmann, S., Solomon, S., Dye, J. E., Baumgardner, D., Kelly, K. K, and Roland Chan K., Heterogeneous reactions on stratospheric background aerosols, volcanic sulfuric acid droplets, and type I polar stratospheric clouds: Effects of temperature fluctuations and differences in particle phase, J. Geophys. Res., 102(D3), 3639-3648, 1997.

Bourassa, A. E., Rieger, L. A., Lloyd, N. D., and Degenstein, D. A.: Odin-OSIRIS stratospheric aerosol data product and SAGE III intercomparison, Atmos. Chem. Phys., 12, 605-614, 2012.

Bracher, A., Sinnhuber, M., Rozanov, A., and Burrows, J. P.: Using a photochemical model for the validation of $NO_2$ satellite measurements at different solar zenith angles, Atmos. Chem. Phys., 5, 393-408, 2005.

Brasseur, G., and C., Granier: Mount Pinatubo aerosols, chlorofluorocarbons and ozone depletion, Science, 257, 1239-1242, 1992.

Brohede, S., McLinden, C. A., Berthet, G., Haley, C. S., Murtagh, D., and Sioris, C. E.: Stratospheric $NO_2$ Climatology from Odin/OSIRIS Limb Scattering Measurements, Can. J. Phys., 85(11), 1253-1274, 2007.

Brohede, S., McLinden, C. A., Urban, J., Haley, C. S., Jonsson, A. I., and Murtagh, D.: Odin stratospheric proxy $NO_y$ measurements and climatology, Atmos. Chem. Phys., 8, 5731–5754, 2008.

Brown, S. S., R. K. Talukdar, and A. R. Ravishankara, Rate constants for the reaction OH + $NO_2$ +M → $HNO_3$ + M under atmospheric conditions, Chem. Phys. Lett., 299, 277– 284, 1999.

Brühl, C., Crutzen, P.J., and Grooss, J.-U.: High-latitude, summertime NOx activation and seasonal ozone decline in the lower stratosphere: Model calculations based on observations by HALOE on UARS, J. Geophys. Res., 103, D3, 3597-3597, 1998.

Bucholtz, A.: Rayleigh-scattering calculations for the terrestrial atmosphere, Appl. Opt., 34, 1227–1230, 1995.

Butz, A., Bösch, H., Camy-Peyret, C., Chipperfield, M., Dorf, M., Dufour, G., Grunow, K., Jeseck, P., Kühl, S., Payan, S., Pepin, I., Pukite, J., Rozanov, A., von Savigny, C., Sioris, C., Wagner, T., Weidner, F., and Pfeilsticker, K.: Inter-comparison of stratospheric $O_3$ and $NO_2$ abundances retrieved from balloon borne direct sun observations and Envisat/SCIAMACHY limb measurements, Atmos. Chem. Phys., 6, 1293–1314, 2006.

Carn, S.A., Clarisse, L. and Prata, A. J.: Multi-decadal satellite measurements of global volcanic degassing, J. Volcanol. Geotherm. Res., 311, 99–134, 2016.

Carslaw, K., Luo, B., and Peter, T.: An analytic expression for the composition of aqueous $HNO_3$-$H_2SO_4$ stratospheric aerosols including gas phase removal of $HNO_3$, Geophys. Res. Lett., 16, 1877-1880, 1995.

Chipperfield, M. P.: Multiannual simulations with a three-dimensional chemical transport model, J. Geophys. Res., 104(D1), 1781-1805, 1999.

Clarisse, L., Hurtmans, D., Clerbaux, C., Hadji-Lazaro, J., Ngadi, Y., and Coheur, P.-F.: Retrieval of sulphur dioxide from the infrared atmospheric sounding interferometer (IASI), Atmos. Meas. Tech., 5, 581–594, doi:10.5194/amt-5-581-2012, 2012.

Cox, R. A., MacKenzie, A. R., Müller, R. H., Peter, T., and Crutzen, P. J.: Activation of stratospheric chlorine by reactions in liquid sulphuric acid, Geophys. Res. Lett., 21(13), 1439-1442, 1994.

Danilin, M. J., Rodriguez, J. M., Hu, W., Ko, M.K.W., Weisenstein, D.K., Kumer, J.B., Mergenthaler, J.L., Russell III, J.M., Koike, M., Yue, G.K., Jones, N.B., and Johnston, P.V.: Nitrogen species in the post-Pinatubo stratosphere: Model analysis utilizing UARS measurements, J. Geophys. Res., 104(D7), 8247-8262, 1999.

Deshler, T., Hervig, M. E., Hofmann, D. J., Rosen, J. M., and Liley, J. B.: Thirty years of in situ stratospheric aerosol size distribution measurements from Laramie, Wyoming (41°N), using balloon-borne instruments, J. Geophys. Res., 108, 4167, doi:10.1029/2002JD002514, 2003.

Dhomse, S. S., Chipperfield, M. P., Feng, W., Hossaini, R., Mann, G. W., and Santee, M. L.: Revisiting the hemispheric asymmetry in midlatitude ozone changes following the Mount Pinatubo eruption: A 3-D model study, Geophys. Res. Lett., 42, 3038-3047, doi:10.1002/2015GL063052.

Dorf, M., Butler, J. H., Butz, A., Camy-Peyret, C., Chipperfield, M. P., Kritten, L., Montzka, S. A., Simmes, B., Weidner, F., and Pfeilsticker, K.: Long-term observations of stratospheric bromine reveal slow down in growth, Geophys. Res. Lett., 33, L24803, doi:10.1029/2006GL027714, 2006a.

Dorf, M., Bösch, H., Butz, A., Camy-Peyret, C., Chipperfield, M. P., Engel, A., Goutail, F., Grunow, K., Hendrick, F., Hrechanyy, S., Naujokat, B., Pommereau, J.-P., Van Roozendael, M., Sioris, C., Stroh, F., Weidner, F., and Pfeilsticker, K.: Balloonborne stratospheric BrO measurements: comparison with Envisat/SCIAMACHY BrO limb profiles, Atmos. Chem. Phys., 6, 2483–2501, 2006b.

Dufour, G., Payan, S., Lefèvre, F., Eremenko, M., Butz, A., Jeseck, P., Té, Y., Pfeilsticker, K., and Camy-Perret, C.: 4-D comparison method to study the $NO_y$ partitioning in summer polar stratosphere – Influence of aerosol burden, Atmos. Chem. Phys., 5, 919–926, 2005.

Erle, F., Grendel, A., Perner, D., Platt, U., and Pfeilsticker, K.: Evidence of heterogeneous chemistry on cold stratospheric sulphate aerosols, Geophys. Res. Lett., Vol. 25, No. 23, 4329-4332, 1998.

Fahey, D. W., Kawa, S. R., Woodbridge, E. L., et al.: In situ measurements constraining the role of sulphate aerosols in mid-latitude ozone depletion, Vol. 363, 509-514, Nature, 1993.

Fahey, D. W., and A. R., Ravishankara: Summer in the stratosphere, Science, 285, n°5425, 208-210, 1999.

Ferlemann, F., Camy-Peyret, C., Fitzenberger, R., Harder, H., Hawat, T., Osterkamp, H., Schneider, M., Perner, D., Platt, U., Vradelis, P., and Pfeilsticker, K.: Stratospheric BrO profiles measured at different latitudes and seasons: Instrument description, spectral analysis and profile retrieval, Geophys. Res. Lett., 25, 3847–3850, 1998.

Ferlemann, F., Bauer, N., Fitzenberger, R., Harder, H., Osterkamp, H., Perner, D., Platt, U., Schneider, M., Vradelis, P., and Pfeilsticker, K.: Differential Optical Absorption Spectroscopy Instrument for stratospheric balloon-borne trace gas studies, Applied Optics, 39, 2377 - 2386, 2000.

Fischer, H. et al.: MIPAS: an instrument for atmospheric and climate research, Atmos. Chem. Phys., 8, 2151-2188, 2008.

Gao, R. S., Fahey, D. W., et al.: A comparison of observations and model simulations of $NO_x/NO_y$ in the lower stratosphere, Geophys. Res. Lett., 26, 1153– 1156, 1999.

Granier., C., and Brasseur, G.: Impact of heterogeneous chemistry on model predictions of ozone changes, J. Geophys. Res., 97(D16), 18,015-18,033, 1992.

Grossel, A., Huret, N., Catoire, V., Berthet, G., Renard, J.-B., Robert, C., and Gaubicher, B.: In situ balloon-borne measurements of $HNO_3$ and HCl stratospheric vertical profiles influenced by PSC formation during 2005-2006 Arctic winter, J. Geophys. Res., 115, D21303, doi: 10.1029/2009JD012947, 2010.

Hanisco, T. F., Lanzendorf, E. J., Wennberg, P. O., Perkins, K. K., Stimpfle, R. M., Voss, P. B., Anderson, J. G. , Cohen, R. C., Fahey, D. W., Gao, R. S., Hintsa, E. J., Salawitch, R. J., Margitan, J. J., McElroy, C. T., and Midwinter, C.: Sources, Sinks, and the Distribution of OH in the Lower Stratosphere, J. Phys. Chem. A, 2001, 105 (9), pp 1543–1553, 2001.

Hanson, D. R., Ravishankara, A. R., and Solomon, S.: Heterogeneous reactions in sulfuric acid aerosols: A framework for model calculations, J. Geophys. Res., 99(D2), 3615-3629, 1994.

Hanson, D. R., and Ravishankara, A. R., Heterogeneous chemistry of bromine species in sulfuric acid under stratospheric conditions, Geophys. Res. Lett., 22(4), 385-388, 1995.

Hanson, D. R., Ravishankara, A. R., and Lovejoy, E. R., Reaction of $BrONO_2$ with $H_2O$ on submicron sulfuric acid aerosol and the implications for the lower stratosphere, J. Geophys. Res., 101(D4), 9063-9069, 1996.

Hanson, D. R., Reactivity of $BrONO_2$ and HOBr on sulfuric acid solutions at low temperatures, J. Geophys. Res., 108(D8), 4239, doi:10.1029/2002JD002519, 2003.

Harder, J.W., Brault, J.W., Johnston, P.V., and Mount, G.H.: Temperature dependent $NO_2$ cross sections at high spectral resolution, J. Geophys. Res., 102, 3861-3879, 1997.

Harder, H., Camy-Peyret, C., Ferlemann, F., Fitzenberger, R., Hawat, T., Osterkamp, H., Perner, D., Platt, U., Schneider, M., Vradelis, P., and Pfeilsticker, K.: Stratospheric BrO Profiles Measured at Different Latitudes and Seasons: Atmospheric Observations, Geophys. Res. Lett., 25, 3843-3846, 1998.

Harder, H., Bösch, H., Camy-Peyret, C, Chipperfield, M., Fitzenberger, R., Payan, S., Perner, D., Platt, U., Sinnhuber, B., and Pfeilsticker, K.: Comparison of measured and modeled stratospheric BrO: Implications for the total amount of stratospheric bromine, Geophys. Res. Lett., 27, 3695 - 3698, 2000.

Harder, J. W., Brault, J. W., Johnston, P. V., and Mount, G. H.: Temperature dependent $NO_2$ cross sections at high spectral resolution, J. Geophys. Res., 102, 3861–3879, 1997.Haywood, J. M., Jones, A., Clarisse, L., Bourassa, A., Barnes, J., Telford, P., Bellouin, N., Boucher, O., Agnew, P., Clerbaux, C., Coheur, P., Degenstein, D., and Braesicke, P.: Observations of the eruption of the Sarychev volcano and simulations using the HadGEM2 climate model, J. Geophys. Res., 115, D21212, doi:10.1029/2010JD014447, 2010.

Haywood, J. M., Jones, A., Clarisse, L., Bourassa, A., Barnes, J., Telford, P., Bellouin, N., Boucher, O., Agnew, P., Clerbaux, C., Coheur, P., Degenstein, D., and Braesicke, P.: Observations of the eruption of the Sarychev volcano and simulations using the HadGEM2 climate model, J. Geophys. Res., 115, D21212, doi:10.1029/2010JD014447, 2010.

Hofmann, D. J., and Solomon, S., Ozone destruction through heterogeneous chemistry following the eruption of El Chichon, J. Geophys. Res., 94(D4), 5029-5041, 1989.

Hofmann, D. J., Oltmans, S. J., Komhyr, W. D., Harris, J. M., Lathrop, J. A., Langford, A. O., Deshler, T., Johnson, B. J., Torress, A, and W. Matthews, A.: Ozone loss in the lower stratosphere over the United States in 1992-1993: Evidence for heterogeneous chemistry on the Pinatubo aerosol, Geophys. Res. Lett., 21(1), 65-68, 1994.

Hormann, C., H. Sihler, N. Bobrowski, S. Beirle, M. Penning de Vries, U. Platt, and T. Wagner, Systematic investigation of bromine monoxide in volcanic plumes from space by using the GOME-2 instrument, Atmos. Chem. Phys., 13, 4749-4781, 2013.

Jégou, F., Berthet, G., Brogniez, C., Renard, J.-B., François, P., Haywood, J.M., Jones, A., Bourgeois, Q., Lurton, T., Auriol, F., Godin-Beekmann, S., Guimbaud, C., Krysztofiak, G., Gaubicher, B., Chartier, M., Clarisse, L., Clerbaux, C., Balois, J.-Y., Verwaerde, C., and Daugeron, D.: Stratospheric aerosols from the Sarychev volcano eruption in the 2009 Arctic summer, Atmos. Chem. Phys., 13, 6533-6552, doi:10.5194/acp-13-6533-2013, 2013.

Johnston, P. V., McKenzie, R. L., Keys, J. G., and Matthews, W. A.: Observations of depleted stratospheric $NO_2$ following the Pinatubo volcanic eruption, Geophys. Res. Lett., 19(2), 211-213, 1992.

Jucks, K. W., Johnson, D. G., Chance, K. V., Traub, W.A., and Salawitch, R. J.: Nitric acid in the middle stratosphere as a function of altitude and aerosol loading, J. Geophys. Res., 104(D21), 26,715-26,723, 1999.

Kinnison, D. E., Grant, K. E., Connell, P. S., Rotman, D. A., and Wuebbles, D. J.: The chemical and radiative effects of the Mount Pinatubo eruption, J. Geophys. Res., 99, D12, 25,705-25,731, 1994.

Koike, M., Kondo, Y., Matthews, W. A., Johnston, P. V., Yamazaki, K.: Decrease of stratospheric $NO_2$ at 44°N caused by Pinatubo volcanic aerosols, Geophys. Res. Lett., 20(18), 1975-1978, 1993.

Koike, M., Jones, N. B., Matthews, W. A., Johnston, P. V., McKenzie, R. L., Kinnison, D., and Rodriguez, J.: Impact of Pinatubo aerosols on the partitioning between $NO_2$ and $HNO_3$, Geophys. Res. Lett., 21(7), 597-600, 1994.

Kondo, Y., Sugita, T., Salawitch, R. J., Koike, M., and Deshler, T.: Effect of Pinatubo aerosols on stratospheric NO, J. Geophys. Res., 102(D1), 1205-1213, 1997.

Kondo, Y., Sugita, T., Koike, M., Kawa, S.R., Danilin, M. Y., Rodriguez, J. M., Spreng, S., Golinger, K., and Arnold, F.: Partitioning of reactive nitrogen in the midlatitude lower stratosphere, J. Geophys. Res., 105(D1), 1417-1424, 2000.

Kravitz, B., Robock, A., Bourassa, A., Deshler, T., Wu, D., Mattis, I., Finger, F., Hoffmann, A., Ritter, C., Bitar, L., Duck, T. J., and Barnes, J. E.: Simulation and observations of stratospheric aerosols from the 2009 Sarychev volcanic eruption, J. Geophys. Res., 116, D18211, doi:10.1029/2010JD015501, 2011.

Krecl, P., Haley, C. S., Stegman, J., Brohede, S. M., and Berthet, G.: Retrieving the vertical distribution of stratospheric OClO from Odin/OSIRIS limb-scattered sunlight measurements, Atmos. Chem. Phys., 6, 1879-1894, 2006.

Kreycy, S. K., Camy-Peyret, C., Chipperfield, M.P., Dorf, M., Feng, W., Hossaini, R., Kritten, L., Werner, B., and Pfeilsticker, K.: Atmospheric test of the J(BrONO2)=k(BrO+NO2) ratio: Implications for total stratospheric $Br_y$ and bromine-mediated ozone loss, Atmos. Chem. Phys., 13, 6263 - 6274, doi:10.5194/acp-13-6263-2013, 2013.

Krysztofiak, G., Thiéblemont, R., Huret, N., Catoire, V., Té, Y., Jégou, F., Coheur, P. F., Clerbaux, C., Payan, S., Drouin, M.A., Robert, C., Jeseck, P., Attié, J.-L., and Camy-Peyret, C.: Detection in the summer polar stratosphere of pollution plume from East Asia and North America by balloon-borne in situ CO measurements, Atmos. Chem. Phys., doi:10.5194/acp-12-11889-2012, 12, 11889–11906, 2012.

Krysztofiak, G., Té, Y. Catoire, V., Berthet, G., Toon, G. C., Jégou, F., Jeseck, P., and Robert, C.: Carbonyl sulfide variability with latitude in the atmosphere, Atmos.-Ocean, 53:1, 89-101, doi: 10.1080/07055900.2013.876609, 2015.

Küll, V., Riese, M., Tie, X., Wiemert, T., Eidmann, G., Offermann, D., and Brasseur, G. P.: $NO_y$ partitioning and aerosol influences in the stratosphere, J. Geophys. Res., Vol. 107, D23, 8183, doi:10.1029/2001JD001246, 2002.

Lary, D. J, Chipperfield, M. P., Toumi, R., and Lenton, T.: Heterogeneous atmospheric bromine chemistry, J. Geophys. Res., 101(D1), 1489-1504, 1996.

Lefèvre, F., Brasseur, G. P., Folkins, I., Smith, A. K., and Simon, P.: Chemistry of the 1991-1992 stratospheric winter : Three-dimensional model simulations, J. Geophys. Res., 99, 9183-8195, 1994.

Lefèvre, F., Figarol, F., Carslaw, K., and Peter, T.: The 1997 Arctic ozone depletion quantified from three-dimensional model simulations, Geophys. Res. Lett., 25, 2425-2428, 1998.

Legras, B., Pisso, I., Berthet, G., and Lefèvre, F.: Variability of the Lagrangian turbulent diffusivity in the lower stratosphere, Atmos. Chem. Phys., 4, 1605–1622, 2005.

Livesey, N.J., et al.: Earth Observing System (EOS) Aura Microwave Limb Sounder (MLS) Version 3.3 and 3.4 Level 2 Data Quality and Description Document. Tech. Rep. JPL D-33509. NASA Jet Propulsion Laboratory, California Institute of Technology, Pasadena, California (91109-8099, available at: http://mls.jpl.nasa.gov/data/datadocs.php), 2011.

McElroy, M. B., Salawitch, R. J., and Minschwaner, K.: The changing stratosphere, Planet. Space. Sci., Vol. 40, No. 2/3, 373-401, 1992.

McGee, T. J., Newman, P., Gross, M., Singh, U., Godin, S., Lacoste, A.-M., and Mégie G., Correlation of ozone loss with the presence of volcanic aerosols, Geophys. Res. Lett., 21(25), 2801-2804, 1994.

Mébarki, Y., Catoire, V., Huret, N., Berthet, G., Robert, C., and Poulet, G.: More evidence for very short-lived substance contribution to stratospheric chlorine inferred from HCl balloon-borne in situ measurements in the tropics, Atmos. Chem. Phys., 10, 1–13, 2010.

Michelsen, H. A., Manney, G. L., Gunson, M. R., and Zander, R.: Correlations of stratospheric abundances of $NO_y$, $O_3$, $N_2O$, and $CH_4$ derived from ATMOS measurements, J. Geophys. Res., 103, 28 347–28 359, 1998.

Michelsen, H. A., Spivakovsky, C.M., and Wofsy, S. C.: Aerosol-mediated partitioning of stratospheric $Cl_y$ and $NO_y$ at temperatures above 200 K, Geophys. Res. Lett., 26(3), 299-302, 1999.

Mills, M. J., Langford, A. O., O'Leary, T. J., Arpag, K., Miller, H. L., Proffitt, M. H., Sander, R. W., and Solomon, S.: On the relationship between stratospheric aerosols and nitrogen dioxide, Geophys. Res. Lett., 20(12), 1187-1190, 1993.

Moreau, G., Robert, C., Catoire, V., Chartier, M., Camy-Peyret, C., Huret, N., Pirre, M., and Pomathiod, L.: A multi-species in situ balloon-borne instrument with six diode laser spectrometers, Appl. Opt., 44(28), 1–18, 2005

Newchurch, M. J., Allen, M., Gunson, M. R., et al.: Stratospheric NO and $NO_2$ abundances from ATMOS solar-occultation measurements, Geophys. Res. Lett., Vol. 23, No. 17, 1996.

O'Neill, N. T., Perro, C., Saha, A., Lesins, G., Duck, T. J., Eloranta, E. W., Nott, G. J., Hoffman, A., Karumudi, M. L., Ritter, C., Bourassa, A., Abboud, I., Carn, S. A., and Savastiouk, V.: Properties of Sarychev sulphate aerosols over the Arctic, J. Geophys. Res., 117, D04203, doi:10.1029/2011JD016838, 2012.

Osterman, G.B., Sen, B. Toon, G.C., Salawitch R.J., Margitan, J.J, and Blavier, J.-F.: Partitioning of $NO_y$ species in the summer Arctic stratosphere, Geophys. Res. Lett., 26(8), 1157-1160, 1999.

Ovarlez J., and Ovarlez, H.: Water vapour and aerosol measurements during SESAME, and the observation of low water vapour content layers, in Polar Stratospheric Ozone, proceedings of the Third European Workshop, Air Pollution Rep. 56, J. A. Pyle, N. R. P. Harris, and G. T. Amanatidis, eds. European Commission, Luxembourg, pp. 205–208, 1995.

Payan, S., Camy-Peyret, C., Jeseck, P., Hawat, T, Pirre, M., Renard, J.-B., Robert, C., Lefèvre, F., Kanzawa, H., and Sasano, Y.: Diurnal and nocturnal distribution of stratospheric $NO_2$ from solar and stellar occultation measurements in the Arctic vortex: comparison with models and ILAS satellite measurements, J. Geophys. Res., 104, 21 585–21 593, 1999.

Pitari, G., and Rizi, V.: An estimate of the chemical and radiative perturbation of stratospheric ozone following the eruption of Mt. Pinatubo, J. Atmos. Sci., Vol. 50, No. 19, 1993.

Pitari, G., Aquila, V., Kravitz, B., Robock, A., Watanabe, S., Cionni, I., De Luca, N., Di Genova, G., Mancini, E., and Tilmes, S.: Stratospheric response to sulfate geoengineering: Results from the Geoengineering Model Intercomparison Project (GeoMIP), J. Geophys. Res., 119, doi:10.1029/2013JD020566, 2014.

Platt, U.: Differential optical absorption spectroscopy (DOAS), in Air Monitoring by Spectroscopic Techniques, M. W. Sigrist, ed., Vol. 127 of Chemical Analysis Series, Wiley, New York, pp. 27–84, 1994.

Pommereau, J.-P., and Piquard, J.: Ozone and nitrogen dioxide vertical distributions by UV-visible solar occultation from balloons, Geophys. Res. Lett., 21, 1227– 1230, 1994.

Portmann, R. W., Brown, S. S., Gierczak, T., Talukdar, R. K., Burkholder, J. B., and Ravishankara, A. R.: Role of nitrogen oxides in the stratosphere: a reevaluation based on laboratory studies, Geophys. Res. Lett., 26(15), 2387-2390, 1999.

Prasad, S. S.: A modeling study of the stratospheric $NO_x/NO_y$ and $NO_x/HNO_3$ ratios : Single- versus dual-channeled mode of OH, $NO_2$ association, J. Geophys. Res., 108, D15, 4474, doi:10.1029/2002JD002970, 2003.

Prather, M.: Catastrophic loss of stratospheric ozone in dense volcanic clouds, J. Geophys. Res., 97, D9, 10,187-10,191, 1992.

Randeniya, L. K., Vohralik, P. F., Plumb, I. C., and Ryan, K. R., Heterogeneous $BrONO_2$ hydrolysis: effect on $NO_2$ columns and ozone at high latitudes in summer, J. Geophys. Res., 102, D19, 23,543-23,557, 1997.

Renard, J.-B., Chartier, M., Robert, C., Chalumeau, G., Berthet, G., Pirre, M., Pommereau, J. P., and Goutail, F.: SALOMON: a new, light balloon borne UV-visible spectrometer for nighttime observations of stratospheric trace-gas species, Appl. Opt., 39, 386–392, 2000.

Renard, J.-B., Taupin, F. G., Rivière, E. D., Pirre, M., Huret, N., Berthet, G., Robert, C., Chartier, M., Pepe, F., and George, M.: Measurements and simulation of stratospheric $NO_3$ at Mid- and High-latitudes in the Northern Hemisphere, J. Geophys. Res., 106, 32387-32399, 2001.

Renard, J.-B., Berthet, G., Robert, C., Chartier, M., Pirre, M., Brogniez, C., Herman, M., Verwaerde, C., Balois, J.-Y., Ovarlez, J., Ovarlez, H., Crespin, J., and Deshler, T.: Optical and physical properties of stratospheric aerosols from balloon measurements in the visible and near-infrared domain: II. Comparison of extinction, reflectance, polarization and counting measurements, Appl. Opt., 41, 7540–7549, 2002.

Renard, J.-B., Ovarlez, J., Berthet, G., Fussen, B., Vanhellemont, F., Brogniez, C., Hadamcik, E., Chartier, M., and Ovarlez, H.: Optical and physical properties of stratospheric aerosols from balloon measurements in the visible and near–infrared domains. III. Presence of aerosols in the middle stratosphere, Appl. Opt., 44, 4086–4095, doi:10.1364/AO.44.004086, 2005.

Renard, J.-B., Brogniez, C., Berthet, G., Bourgeois, Q., Gaubicher, B., Chartier, M., Balois, J.-Y., Verwaerde, C., Auriol, F., François, P., Daugeron, D., and Engrand, C.: Vertical distribution of the different types of aerosols in the stratosphere, Detection of solid particles and analysis of their spatial variability, J. Geophys. Res., 113, D21303, doi:10.1029/2008JD010150, 2008.

Renard, J.-B., Berthet, G, Salazar, S., Catoire, V., Tagger, T., Gaubicher, B., and Robert, C: In situ detection of aerosol layers in the middle stratosphere, Geophys. Res. Lett., 37, L20803, doi:10.1029/2010GL044307, 2010.

Rinsland, C. P., Weisenstein, D. K., Ko, M. K. W., Scott, C. J., Chiou, L. S., Mahieu, E., Znader, R., and Demoulin, P.: Post-Mount Pinatubo eruption ground-based infrared stratospheric column measurements of $HNO_3$, NO, and $NO_2$ and their comparison with model calculations, J. Geophys. Res., 108, D15, doi:10.1029/2002JD002965, 2003.

Rivière, E. D., Pirre, M., Berthet, G., Renard, J.-B., and Lefèvre, F.: Investigating the OClO and $Br_y$ chemistry from high-latitude nighttime measurements of OClO and $NO_2$, J. Atmos. Chem., 48, 261-282, 2004.

Robock, A.: Volcanic eruptions and climate, Rev. Geophys., 38, 2, 191-219, 2000.

Rodgers, C.: Inverse methods for atmospheric sounding: theory and practice, xvi-238 p.:ill., World scientific publishing, 2000.

Rodriguez, J. M., Ko, M. K. W., and Sze N. D., Role of heterogeneous conversion of $N_2O_5$ on sulphate aerosols in global ozone losses, Nature, 352, 134-137, 1991.

Rothman, L. S., Gordon, I. E., Babikov, Y., Barbe, A., Benner, D. C., Bernath, P. F., et al.: The HITRAN2012 molecular spectroscopic database, J. Quant. Spectrosc. Radiat. Transfer, 130, 4–50, doi:10.1016/j.jqsrt.2013.07.002, 2013.

Salawitch, R. J., Wofsy, S. C., Wennberg, P. O., et al.: The distribution of hydrogen, nitrogen, and chlorine radicals in the lower stratosphere: Implications for changes in $O_3$ due to emission of $NO_y$ from supersonic aircraft, Geophys. Res. Lett., 21(23), 2547-2550, 1994a.

Salawitch, R. J., Wofsy, S. C., Wennberg, P. O., et al., The diurnal variation of hydrogen, nitrogen, and chlorine radicals: Implications for the heterogeneous production of $HNO_2$, Geophys. Res. Lett., 21(23), 2551-2554, 1994b.

Salawitch, R. J., Weisenstein, D. K., Kovalenko, L. J., Sioris, C. E., Wennberg, P. O., Chance, K., Ko, M. K. W., and McLinden, C. A.: Sensitivity of ozone to bromine in the lower stratosphere, Geophys. Res. Lett., 32, L05811, doi:10.1029/2004GL021504, 2005.

Sander, S. P., Abbatt, J. P. D., Friedl, R. R., Barker, J. R., Burkholder, J. B., Golden, D. M., Kolb, C. E., Kurylo, M. J., Moortgat, G. K., Wine, P. H., Huie, R. E., Orkin, V. L.: Chemical kinetics and photochemical data for use in atmospheric studies, Evaluation number 17, JPL Publ., 10-6, 684 pp., 2011.

Santee, M. L., Manney, G. L., Livesey, N. J., and Read, W. G.: Three-dimensional structure and evolution of stratospheric $HNO_3$ based on UARS Microwave Limb Sounder measurements, 109, D15306, doi:10.1029/2004JD004578, 2004.

Sen, B., Toon, G. C., Osterman, G. B., Blavier, J.-F., Margitan, J. J., Salawitch, R. J., and Yue, G. K.: J. Geophys. Res., 103, D3, 3571-3585, 1998.

Shi, Q., Jayne, J. T., Kolb, C. E., and Worsnop, D. R.: Kinetic model for reaction of $ClONO_2$ with $H_2O$ and HCl and HOCl with HCl in sulfuric acid solutions, J. Geophys. Res., 106, D20, 24,259-24,274, 2001.

Solomon, S. Sanders, R. W., Jakoubek, R. O., Arpag, K. H., Stephens, S. L., Keys, J. G., and Garcia, R. R.: Visible and near-ultraviolet spectroscopy at McMurdo Station, Antarctica. 10. Reductions of stratospheric $NO_2$ due to Pinatubo aerosols, J. Geophys. Res., 99(D2), 3509-3516, 1994.

Solomon, S., Portmann, R. W., Garcia, R. R., Thomason, L. W., Poole, L. R., and McCormick, M. P.: The role of aerosol variations in anthropogenic ozone depletion at northern midlatitudes, J. Geophys. Res., 101(D3), 6713-6727, 1996.

Solomon, S., Stratospheric ozone depletion: a review of concepts and history, Rev. Geophys., 37, 3, 275-316, 1999.

Solomon, S., Ivy, D. J., Kinnison, D., Mills, M. J., Neely III, R. R., and Schmidt, A.: Emergence of healing in the Antarctic ozone layer, Science, Vol. 353, Issue 6296, 2016.

Steele, H. M., and R. P., Turco, Retrieval of aerosol size distributions from satellite extinction spectra using constrained linear inversion, J. Geophys. Res., 102(D14), 16,737-16,747, 1997.

Stutz, J., and Platt, U.: Numerical analysis and estimation of the statistical error of differential optical absorption spectroscopy measurements with least squares methods, Appl. Optics, 35, 6041-6053, 1996.

Swartz, W. H., Yee, J.-H., Randall, C. E., Shetter, R. E., Browell, E. V., Burris, J. F., McGee, T. J., and Avery, M. A.: Comparison of high latitude line of sight ozone column density with derived ozone fields and the effects of horizontal inhomogeneity, Atmos. Chem. Phys., 6, 1843– 1852, 2006.

Tabazadeh, A., Toon, O. B., Clegg, S. L., and Hamill, P.: A new parameterization of $H_2SO_4/H_2O$ aerosol composition: Atmospheric implications, Geophys. Res. Lett., 24, 1931-1934, 1997.

Telford, P., Braesicke, P., Morgenstern, O., and Pyle, J.: Reassessment of causes of ozone column variability following the eruption of Mount Pinatubo using a nudged CCM, Atmos. Chem. Phys., 9, 4251–4260, 2009.

Tie, X., Brasseur, G. P., Briegleb, B., and Granier, C., Two-dimensional simulation of Pinatubo aerosol and its effect on stratospheric ozone, J. Geophys. Res., 99, D10, 20,545-20,562, 1994.

Tie, X., and Brasseur, G.: The response of stratospheric ozone to volcanic eruptions: Sensitivity to atmospheric chlorine loading, Geophys. Res. Lett., Vol. 22, No. 22, 3035-3038, 1995.

Tie, X., and Brasseur, G. P.: The importance of heterogeneous bromine chemistry in the lower stratosphere, Geophys. Res. Lett., Vol. 23, No. 18, 2505-2508, 1996.

Van de Hulst, H. C.: Light Scattering By Small Particles, JohnWiley & Sons, Inc., New York, 1957.

Vernier, J.-P., Thomason, L. W., Pommereau, J.-P., Bourassa, A., Pelon, J., Garnier, A., Hauchecorne, A., Blanot, L., Trepte, C., Degenstein, D., and Vargas, F.: Major influence of tropical volcanic eruptions on the stratospheric aerosol layer during the last decade, Geophys. Res. Lett., 38, L12807, doi:10.1029/2011GL047563, 2011.

Wahner, A., Ravishankara, A., Sander, S., and Friedl, R.: Absorption cross section of BrO between 312 and 385 nm at 298 and 223 K, Chem. Phys. Lett., 152, 507–512, 1988.

Webster, C. R., May, R. D., Allen, M., Jaeglé, L., and McCormick M. P.: Balloon profiles of stratospheric $NO_2$ and $HNO_3$ for testing the heterogeneous hydrolysis of $N_2O_5$ on sulfate aerosols, Geophys. Res. Lett., Vol. 21, No. 1, 53-56, 1994.

Webster, C. R., May, R. D., Michelsen, H. A., et al.: Evolution of HCl concentrations in the lower stratosphere from 1991 to 1996 following the eruption of Mt. Pinatubo, Geophys. Res. Lett., 25(7), 995-998, 1998.

Webster, C. R., Michelsen, H. A., Gunson, M. R., Margitan, J. J., Russell III, J. M., Toon, G. C., and Traub, W. A., J.: Response of lower stratospheric $HCl/Cl_y$ to volcanic aerosols: Observations from aircraft, balloon, space shuttle, and satellite instruments, Geophys. Res., 105, D9, 11,711-11,719, 2000.

Weisenstein, D. K., Ko, M. K. W., Rodriguez, J. M., and N.-D. Sze.: Impact of heterogeneous chemistry on model-calculated ozone change due to high speed civil transport aircraft, Geophys. Res. Lett., Vol. 18, No. 11, 1991-1994, 1991.

Weisenstein, D. K., and Bekki, S.: Modeling of stratospheric aerosols, Assessment of Stratospheric Aerosol Properties (ASAP), Chapter 6, WCRP-124, WMO/TD- No. 1295, SPARC Report No. 4, 2006.

Wennberg, P. O., Cohen, R. C., Stimpfle, R. M., et al.: Removal of stratospheric $O_3$ by radicals: in situ measurements of OH, $HO_2$, NO, $NO_2$, ClO and BrO, Science, 266, 398-404, 1994.

Wennberg, P. O., Hanisco, T. F., Cohen, R. C., Stimpfle R. M., Lapson, L. B. and Anderson, J .G.: In situ measurements of OH and $HO_2$ in the upper troposphere and stratosphere, J. Atmos. Sci., Vol. 52, No. 19, 3413-3420, 1995.

Wetzel, G., Oelhaf, H., Ruhnke, R., Friedl-Vallon, F., Kleinert, A., Kouker, W., Maucher, G., Reddmann, T., Seefeldner, M., Stowasser, M., Trieschmann, O., Von Clarmann, T., and Fischer, H.: $NO_y$ partitioning and budget and its correlation with $N_2O$ in the Arctic vortex and in summer midlatitudes in 1997, J. Geophys. Res., 107(D16), doi:10.1029/2001JD000916, 2002.

Willeke, K. and Liu, B. Y. H.: Single particle optical counter: principle and application, in Fine Particles, Aerosol Generation, Measurement, Sampling and Analysis, B. Y. H. Liu, ed. Academic, Orlando, Fla., 698–729, 1976.

Wiscombe, W. J.: Improved Mie scattering algorithms, Appl. Opt., 19, 1505– 1509, 1980.

World Meteorological Organization (WMO): Scientific Assessment of Ozone Depletion, Report No 52, Geneva, 2010.

World Meteorological Organization (WMO): Scientific Assessment of Ozone Depletion, Report No 55, Geneva, 2014.

**Table 1**: Simulated changes on various stratospheric key species due to the Sarychev volcanic aerosols over the August-September 2009 period at 16.5 km. Numbers are taken from the Sat-sim simulation. Effects for daytime and night-time conditions are provided depending on statistically significant amounts in the diurnal cycle of a given compound. Also the contribution of $BrONO_2$ hydrolysis (reaction 4) to changes on the various species is shown (see text).

| Species | All chemistry | | | | $BrONO_2$ hydrolysis effect | |
|---|---|---|---|---|---|---|
| | 12H UT | | 00H UT | | 12H UT | 00H UT |
| $NO_x$ | -0.23 ppbv | -44% | -0.19 ppbv | -48% | 1.8% | 1.1% |
| $NO_2$ | -0.12 ppbv | -43% | -0.19 ppbv | -48% | 1.8% | 1.1% |
| NO | -0.11 ppbv | -45% | --- | --- | 2.0% | --- |
| $HNO_3$ | +0.31 ppbv | +11% | +0.31 ppbv | +11% | -2.3% | -0.9% |
| $N_2O_5$ | -0.08 ppbv | -80% | -0.12 ppbv | -66% | -3.6% | -3.1% |
| $ClONO_2$ | +0.02 ppbv | +16% | +0.02 ppbv | +22% | 66.2% | 60.6% |
| HCl | -0.02 ppbv | -3% | -0.02 ppbv | -3% | 58.8% | 58.9% |
| $ClO_x$ | +5.77 pptv | +106% | --- | --- | 39.3% | --- |
| ClO | +5.77 pptv | +106% | --- | --- | 39.3% | --- |
| HOCl | +2.17 pptv | +217% | +1.16 pptv | +346% | 47.4% | 50.1% |
| $BrONO_2$ | -1.37 pptv | -33% | -4.15 pptv | -70% | 18.3% | 98% |
| BrO | +0.94 pptv | +22% | --- | --- | 16.2% | --- |
| HOBr | --- | --- | +3.89 pptv | +141% | --- | 98.8% |
| $HO_x$ | +1.41 pptv | +51% | --- | --- | 24.1% | --- |
| OH | +0.05 pptv | +16% | --- | --- | 44.1% | --- |
| $HO_2$ | +1.36 pptv | +56% | --- | --- | 23.1% | --- |
| $O_3$ | -13.1 ppbv | -1.1% | -12.6 ppbv | -1.1% | 22.5% | 26.3% |

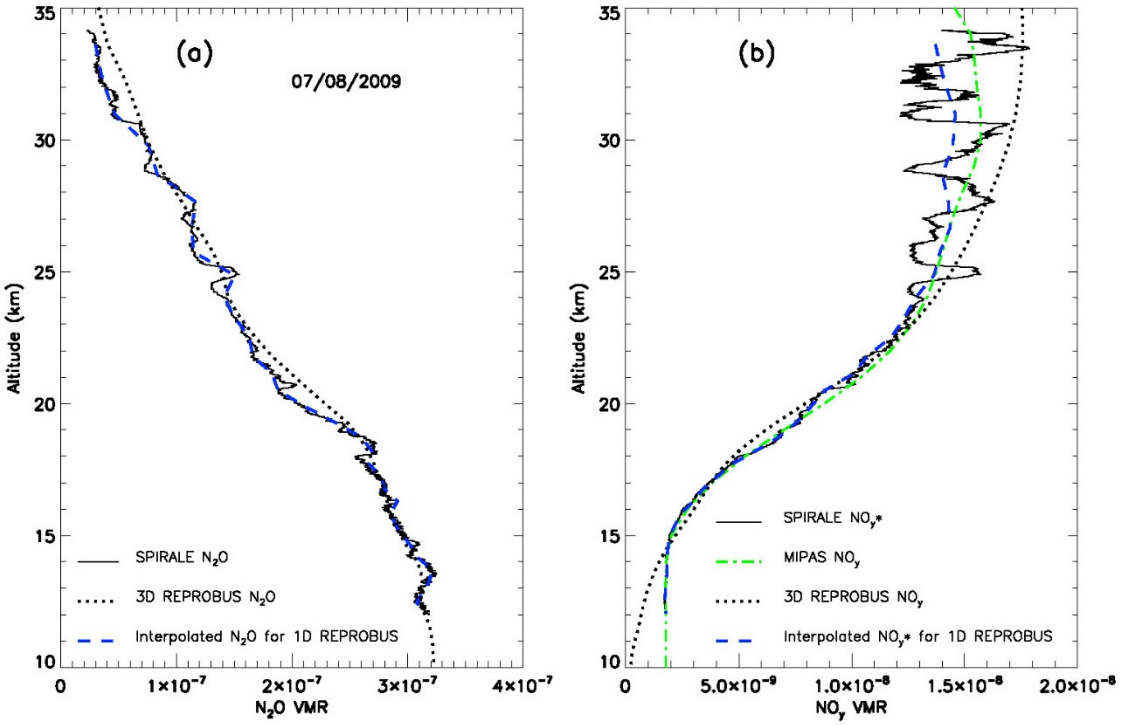


**Figure 1:** (a) Vertical profile of $N_2O$ recorded on 7 August 2009 (black line) compared to the results from the 3D version of REPROBUS (dotted line). (b) Vertical profile of $NO_y$ inferred from the SPIRALE $N_2O$ profile converted using the $N_2O$-$NO_y$ correlation curve presented in **Figure 7** (referred to as $NO_y$*). Also shown are the $NO_y$ profiles from the 3D version of REPROBUS (dotted line) and the MIPAS averaged data (green line). The 1D version of REPROBUS is computed with the profiles interpolated to the model resolution (blue lines).

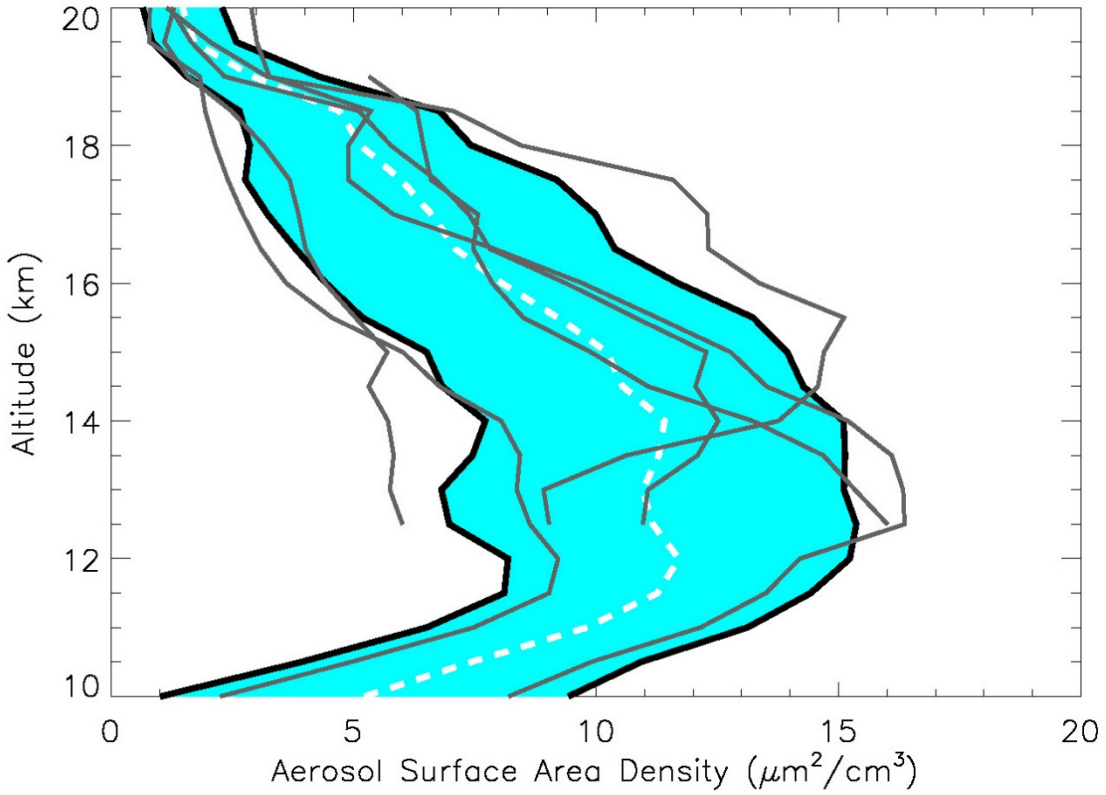


**Figure 2:** Range of aerosol SAD values (black lines) as derived from several balloon-borne observations in the lower stratosphere in summer 2009 (1σ standard deviation of the mean). The individual profiles (grey lines) and their average (white dashed line) are also presented. Data supposed to be spoiled by balloon outgassing as revealed from simultaneous in situ water vapour observations and data revealing the sporadic presence of clouds below 12 km have been excluded.

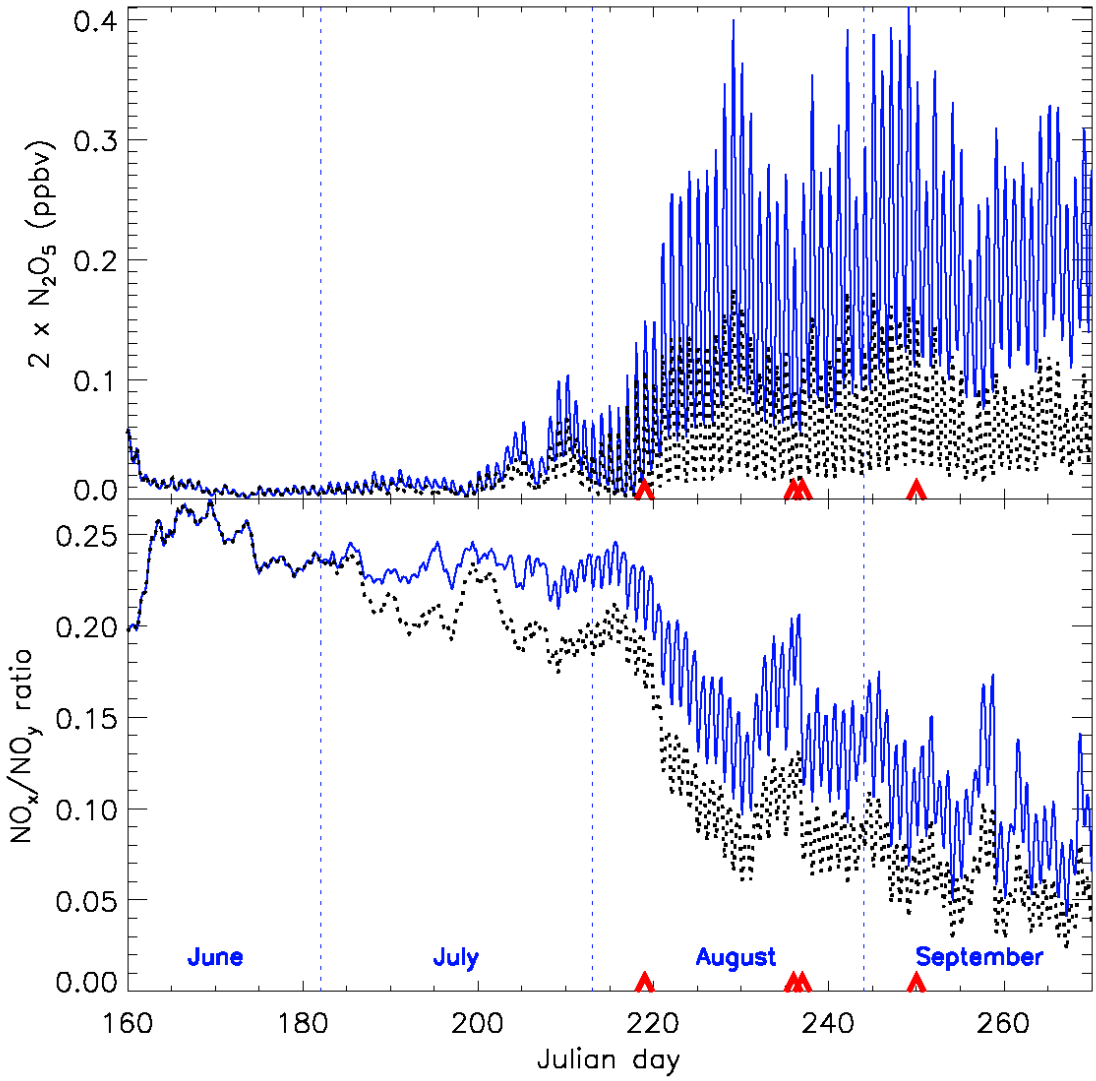


**Figure 3**: Seasonal variation of $N_2O_5$ (a) and of the $NO_x/NO_y$ ratio (b) simulated by the REPROBUS CTM above Kiruna in Northern Sweden (67.5°N, 21.0°E) around 17.5 km. The simulation driven by non-volcanic aerosol contents (Ref-sim) is shown in blue. The black dotted line is the REPROBUS simulation driven by volcanic aerosol levels from STAC balloon-borne observations (Bal-sim). Red triangles represent the dates of the balloon flights. $N_2O_5$ recovery is onset at the beginning of August (day 213 is August 1, 2009) i.e. when SZA become >90°.

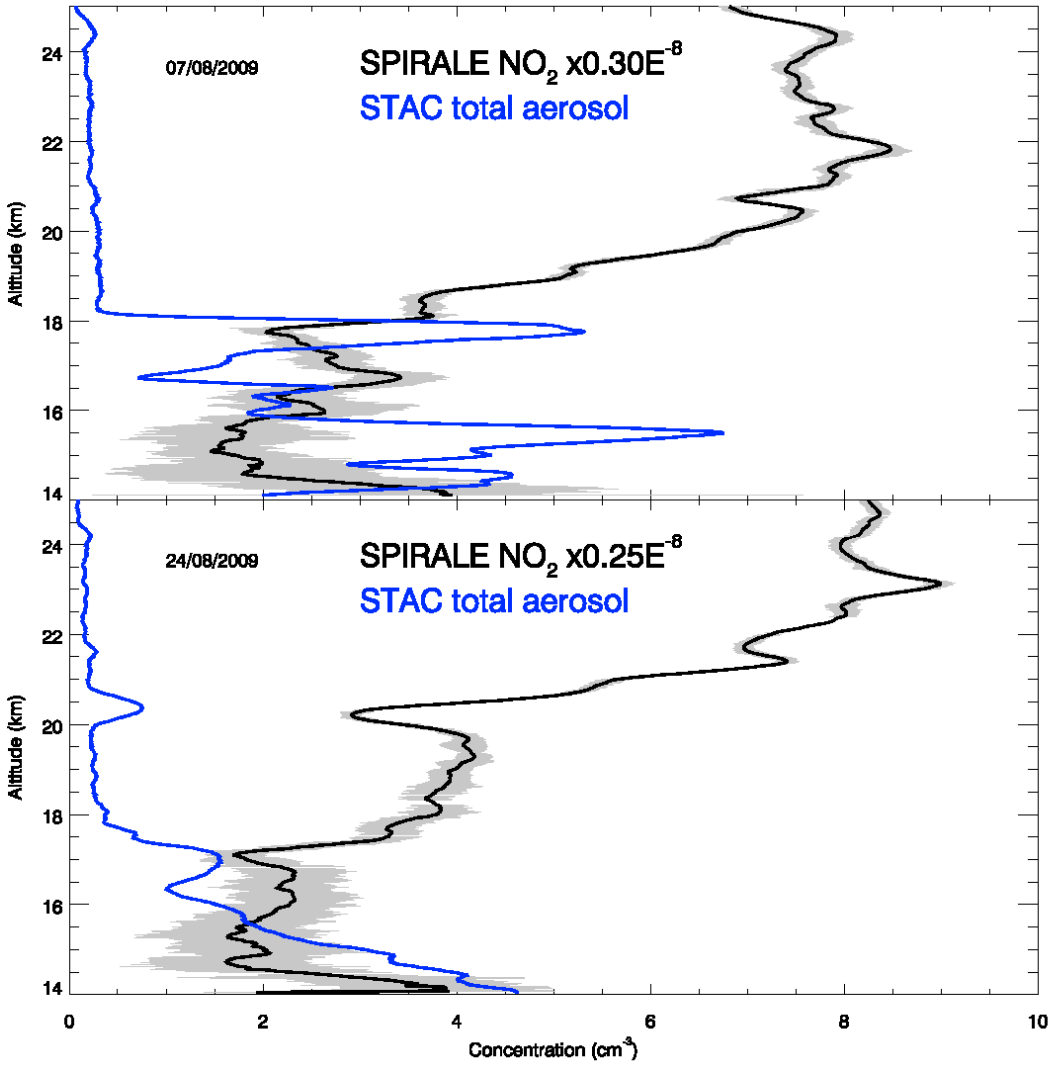


**Figure 4:** Vertical profiles of $NO_2$ observed by the SPIRALE balloon-borne instrument (black line with grey shaded error bars) on 7 and 24 August 2009 compared to the total aerosol concentration profiles (for sizes > 0.4 µm) simultaneously recorded by the STAC aerosol counter (blue line) above Kiruna during balloon ascent. SPIRALE data have been averaged over 250 m (corresponding to ~1 minute of measurements).

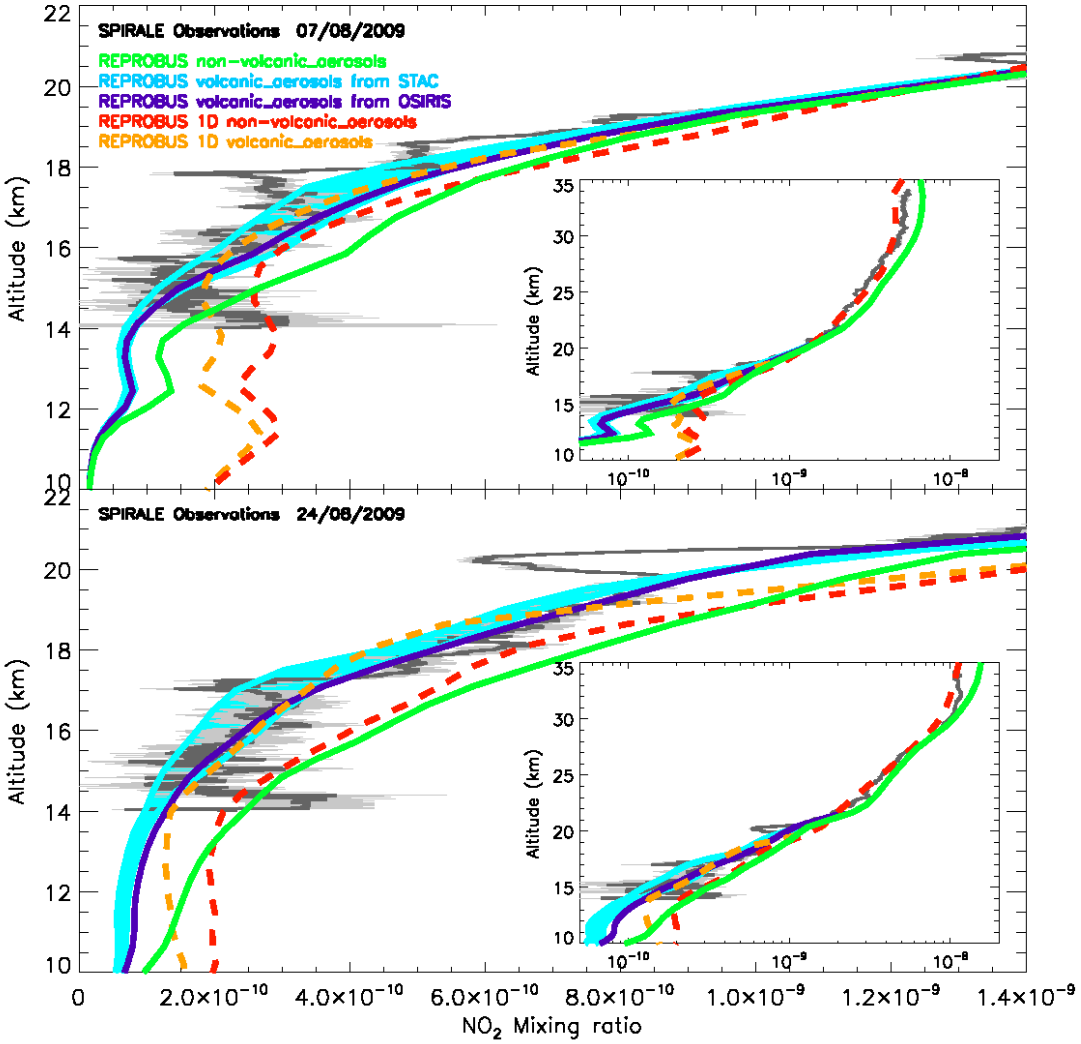


**Figure 5:** Vertical profile of $NO_2$ observed by the SPIRALE balloon-borne instrument (black line) above Kiruna during balloon ascent between 02:00 and 02:30 UT (~87° SZA at 02:15 UT) for the 7 August 2009 flight (top) and between 21:00 and 21:30 UT (~100° SZA at 21:15 UT) for the 24 August 2009 flight (bottom). Model outputs (available every 15 minutes) are provided for the closest location of the instrument and interpolated to the time of observations. Three-dimensional simulations have been driven without volcanic aerosols (green), with volcanic aerosols from balloon-borne observations (blue shaded area) and with volcanic aerosols from satellite data (dark blue line). Results from a one-dimensional (1D) version of the REPROBUS model (dashed lines) computed using hybrid $NO_y$ profiles ($NO_y$*) derived from the observed profiles of $N_2O$ are also provided (see text), with in red the non-volcanic reference simulations and in yellow the calculations driven with volcanic aerosols from the mean observed balloon-borne profile presented in **Figure 2**.

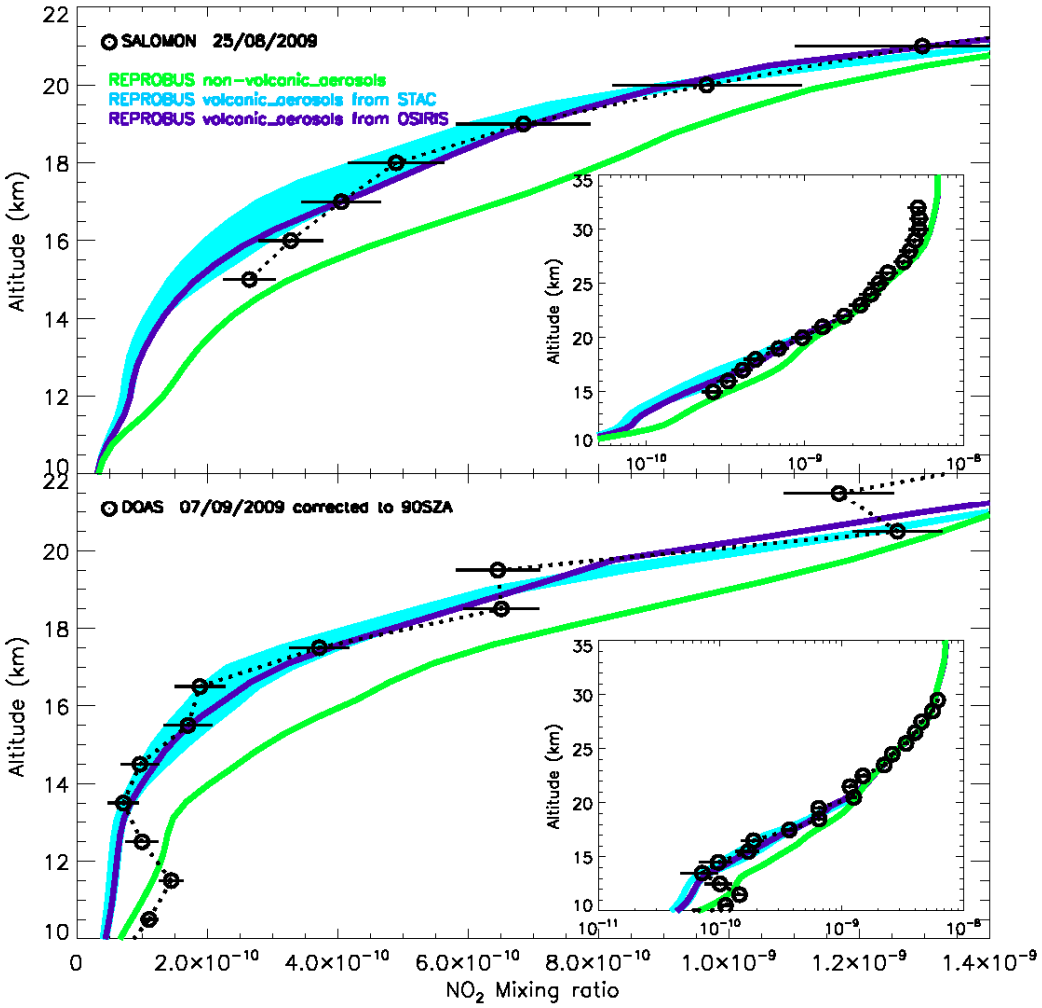


**Figure 6:** (top) Vertical profile of $NO_2$ recorded by the SALOMON instrument (black lines) obtained during solar occultation between 18:50 (32 km tangent height) and 19:30 UT (15 km tangent height) on 25 August 2009 above Kiruna. Chemistry-transport model simulations computed with no volcanic aerosols (green line), with volcanic aerosols from balloon-borne observations (blue shaded area) and with volcanic aerosols from satellite data (dark blue line) are shown. The model output is provided for the closest location of the tangent points. (bottom) Vertical profile of $NO_2$ recorded by the DOAS instrument (black lines) on 7 September 2009 above Kiruna. The DOAS profile has been recorded during the balloon ascent and has been converted to 90°SZA (~17:30 UT) as well as the simulated profile.

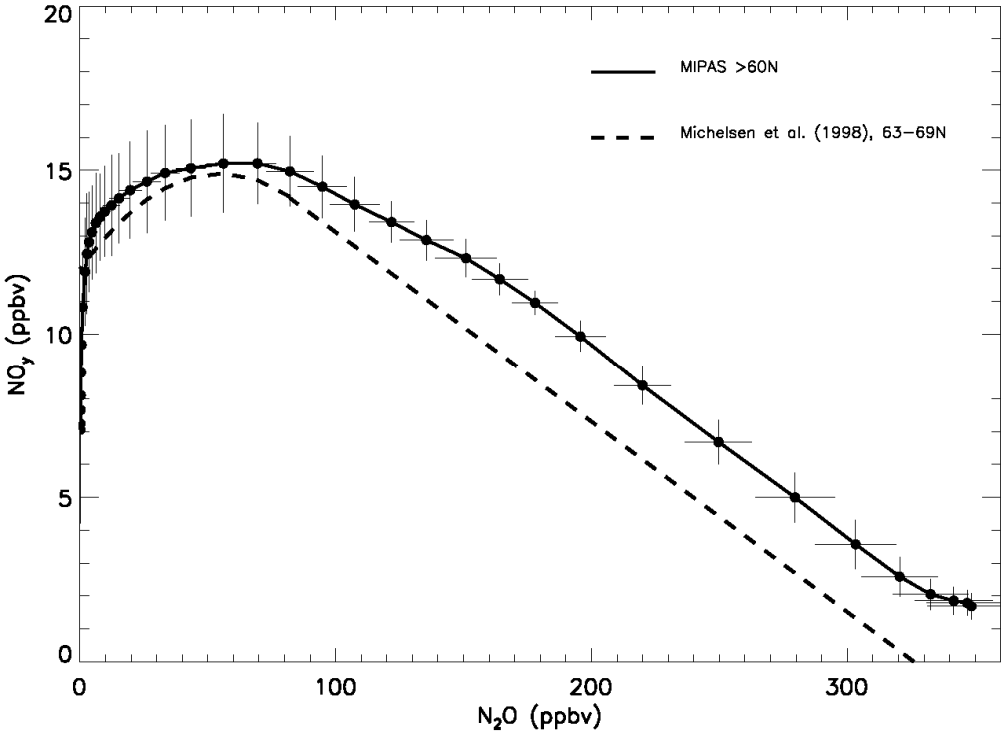


**Figure 7:** $N_2O$-$NO_y$ correlation curve inferred from IMK/IAA V5R_220 MIPAS-Envisat data at high latitudes (> 60°N) in July-August 2009 (full line). Error bars reflect the spread of the data. The former Michelsen et al. (1998) correlation is also shown for comparison (dashed line).

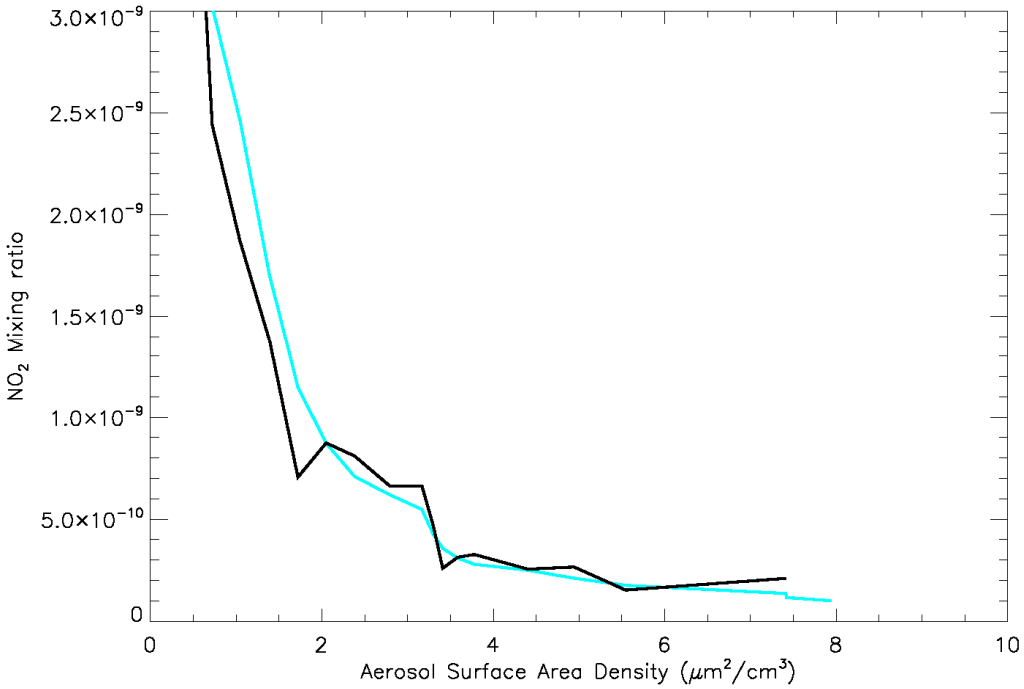


**Figure 8**: $NO_2$ mixing ratio as a function of aerosol SAD as simultaneously observed in the lower stratosphere by the SPIRALE and STAC instruments on 24 August 2009 (black curve). The result from the REPROBUS Bal-sim simulation is also plotted (blue curve).

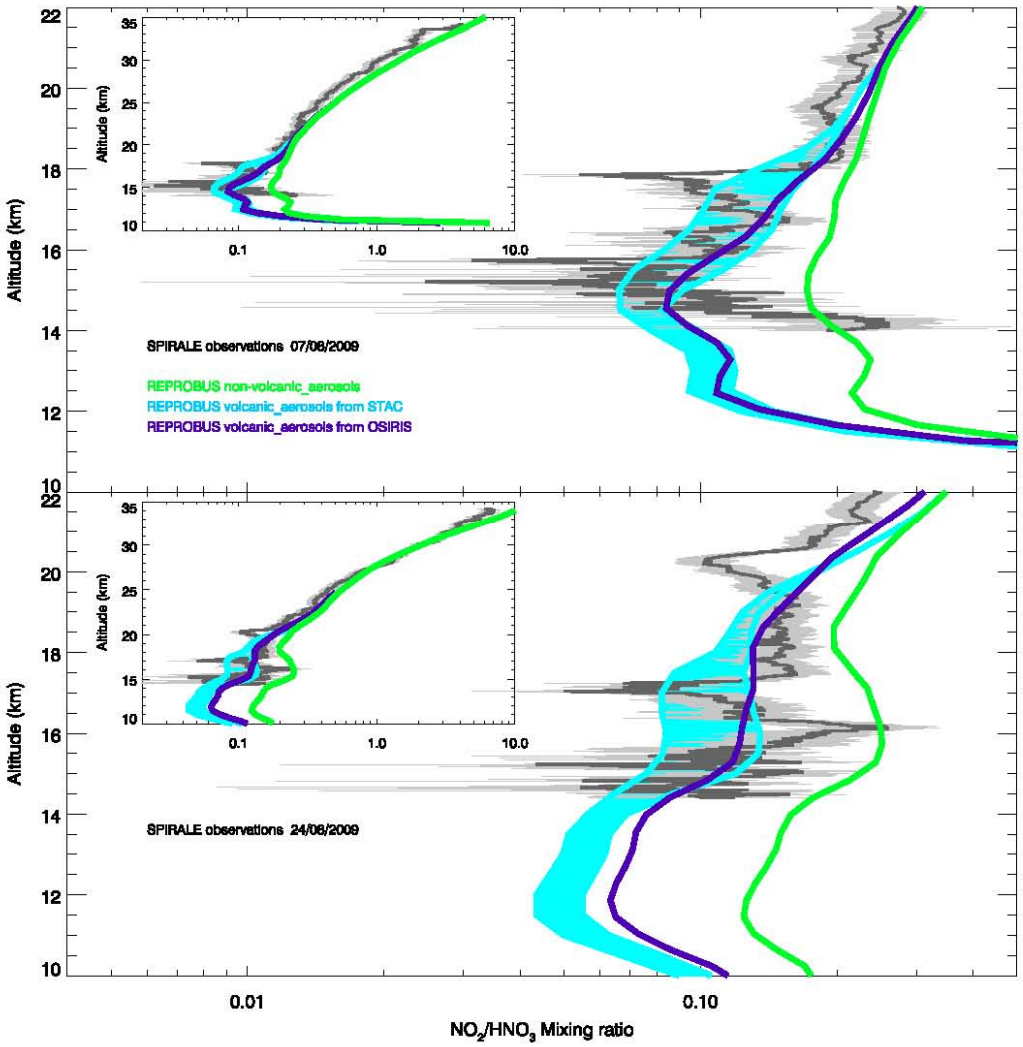


**Figure 9:** Same as **Figure 5** but for the $NO_2/HNO_3$ ratio observed by the SPIRALE instrument. Provided are the three-dimensional simulations driven without volcanic aerosols (green), with volcanic aerosols from balloon-borne observations (blue shaded area) and with volcanic aerosols from satellite data (dark blue line).

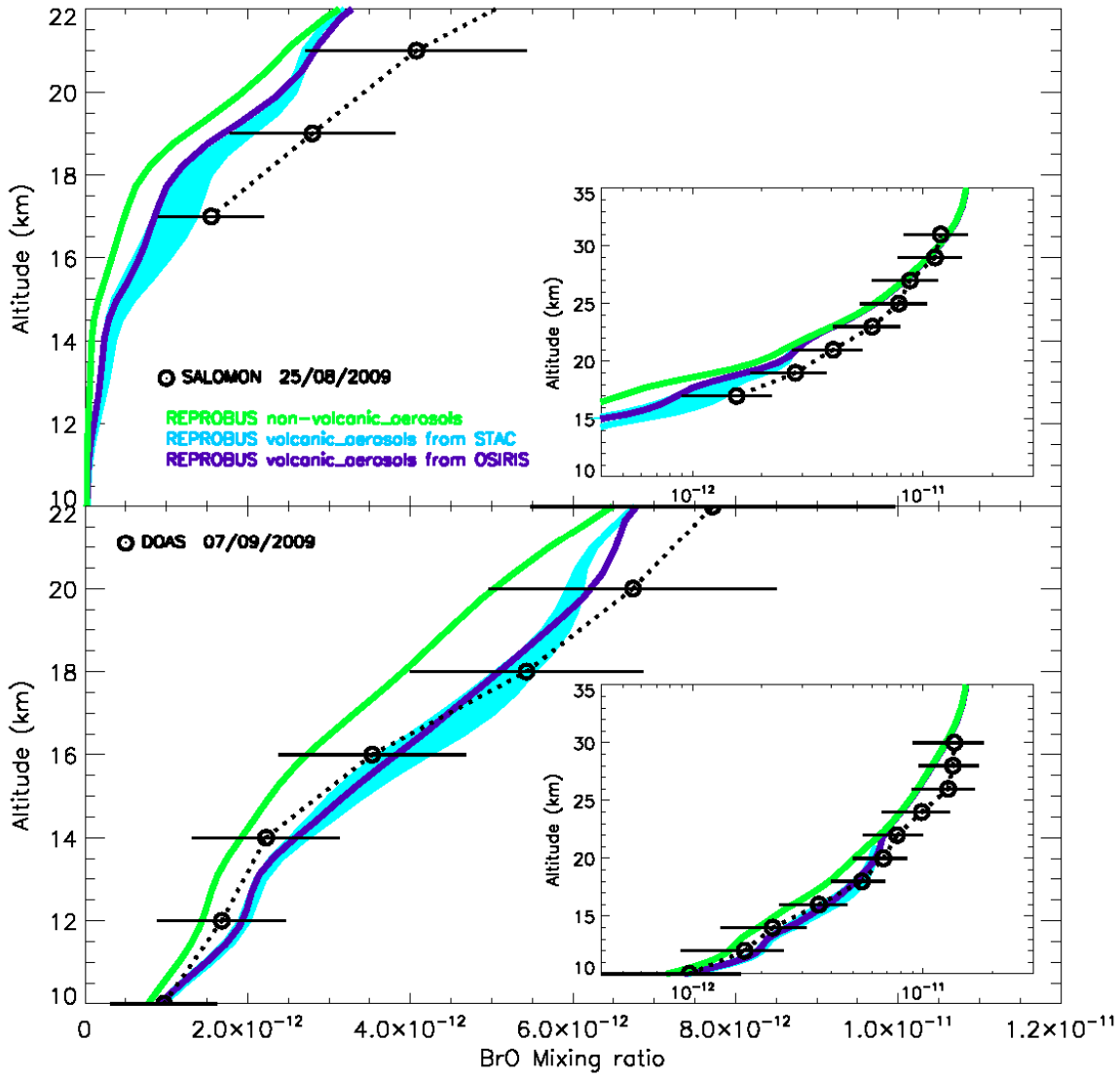


**Figure 10:** same as **Figure 6** but for BrO. The SALOMON data in the lower stratosphere were obtained between 19:15 UT (SZA=93.8° at 22 km tangent height) and 19:25 UT (SZA=94.5° at 17 km tangent height). The DOAS profile was measured between 15:15 UT (SZA=77.5° at 10 km) and 15:55 UT (SZA=81.3° at 22 km) during balloon ascent.

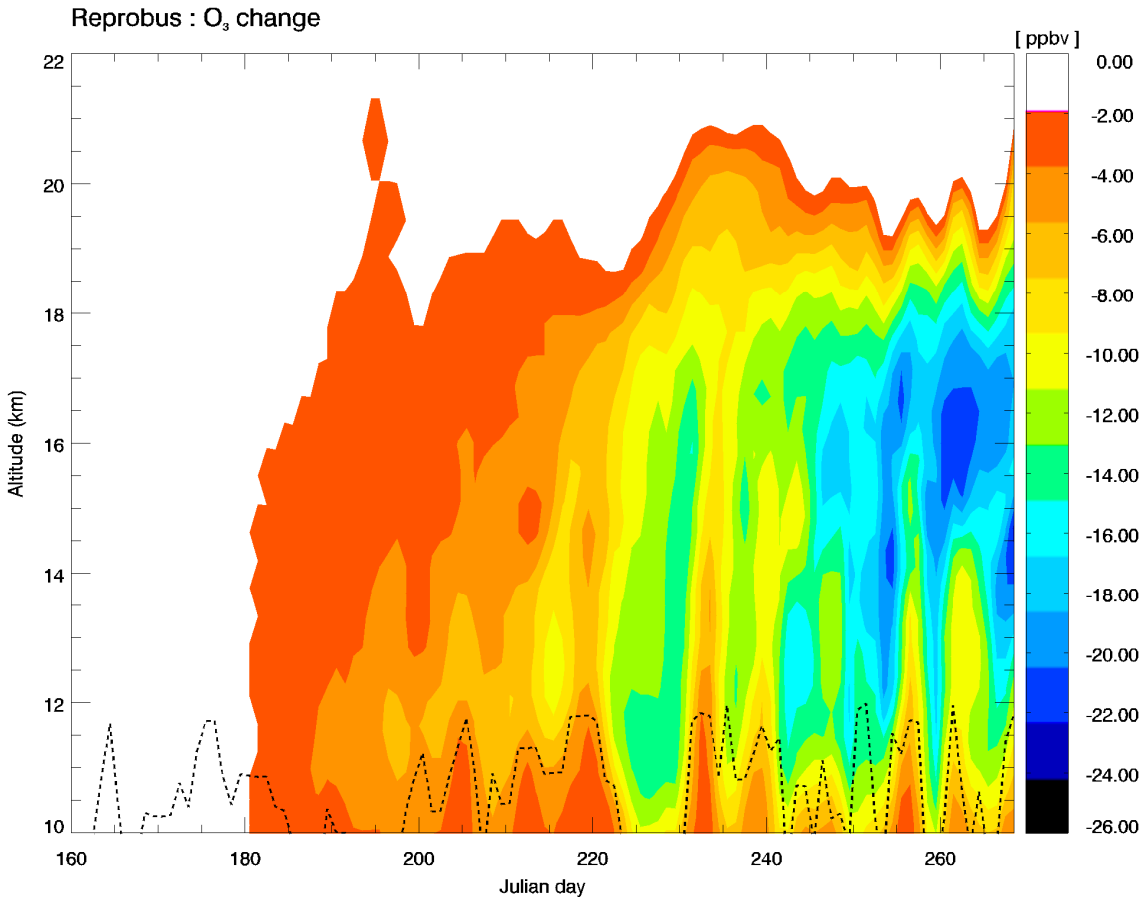


**Figure 11**: Changes in ozone over Kiruna (67.5°N, 21.0°E) as a function of altitude and time between 1 July and 1 October 2009. Calculations are done by subtracting outputs from the volcanic simulation driven by OSIRIS observations with the background simulation. The position of the tropopause is given by the black dotted line.